

# Finiteness of Stationary Configurations of the Planar Four-vortex Problem. II

Xiang Yu\*

*School of Economic and Mathematics, Southwestern University of Finance and Economics,  
Chengdu 611130, China*

## Abstract

In an earlier paper [16], we showed that there are finitely many stationary configurations (consisting of equilibria, rigidly translating configurations, relative equilibria and collapse configurations) in the planar four-vortex problem. However, we only established finiteness of collapse configurations in the sense of prescribing a collapse constant. In this paper, by developing ideas of Albouy-Kaloshin and Hampton-Moeckel to do an analysis of the singularities, we further show that there really are finitely many collapse configurations in the four-vortex problem. This is an unexpectedly result, because the  $N$ -vortex problem has infinitely many collapse configurations for  $N = 3$  and for  $N = 5$ . We also provide better upper bounds for collapse configurations than that in [16].

**Key Words:** Point vortices; Self-similar solutions; Bézout theorem.

**2020AMS Subject Classification:** 76B47 70F10 70F15 37Nxx.

## Contents

<b>1</b>	<b>Introduction</b>	<b>2</b>
<b>2</b>	<b>Preliminaries</b>	<b>5</b>
2.1	Stationary configurations . . . . .	5
2.2	Complex central configurations . . . . .	7
2.3	Elimination theory . . . . .	8
2.4	Bézout Theorem . . . . .	9
<b>3</b>	<b>Puiseux series solutions and colored diagram</b>	<b>9</b>
3.1	Notations and definitions . . . . .	10
3.2	New normalization. Main estimates. . . . .	12

---

\*Email: xiang.zhiy@foxmail.com, xiang.zhiy@gmail.com

<b>4</b>	<b>Possible diagrams in the case <math>q &lt; - \gamma /2</math></b>	<b>13</b>
4.1	Possible diagrams . . . . .	13
4.2	Exclusion of diagrams . . . . .	17
4.3	Problematic diagrams . . . . .	18
4.3.1	Diagram I . . . . .	18
4.3.2	Diagram II . . . . .	19
4.3.3	Diagram III . . . . .	20
<b>5</b>	<b>Possible diagrams in the case <math>q = - \gamma /2</math></b>	<b>21</b>
5.1	The case that some $w_n \prec t^{-\frac{\gamma}{2}}$ . . . . .	21
5.1.1	Possible diagrams . . . . .	21
5.1.2	Exclusion of diagrams . . . . .	22
5.2	The case that all $w_n \approx t^{-\frac{\gamma}{2}}$ . . . . .	24
5.2.1	Possible diagrams . . . . .	24
5.2.2	Exclusion of diagrams . . . . .	24
5.3	Problematic diagrams . . . . .	27
<b>6</b>	<b>Finiteness results of collapse configurations</b>	<b>27</b>
6.1	Finiteness of collapse configurations except two special cases . . . . .	33
6.2	Finiteness of collapse configurations in case $\Gamma_1 = \Gamma_2 = \Gamma_3 = -\Gamma_4$ . . . . .	35
6.3	Finiteness of collapse configurations in case $\Gamma_3 = \Gamma_4 = (\sqrt{3} - 2)\Gamma_1 =$ $(\sqrt{3} - 2)\Gamma_2$ . . . . .	35
<b>7</b>	<b>Upper bounds on the number of <math>\Lambda</math> and on collapse configurations</b>	<b>37</b>
<b>8</b>	<b>Conclusion</b>	<b>41</b>

# 1 Introduction

We consider the motion of  $N$  point vortices on a plane, the so-called  $N$ -vortex problem introduced by Helmholtz [10]. The equations of motion of the  $N$ -vortex problem are written as

$$\Gamma_n \dot{\mathbf{r}}_n = J \sum_{1 \leq j \leq N, j \neq n} \frac{\Gamma_n \Gamma_j (\mathbf{r}_j - \mathbf{r}_n)}{|\mathbf{r}_j - \mathbf{r}_n|^2}, \quad n = 1, 2, \dots, N. \quad (1.1)$$

where  $J = \begin{pmatrix} 0 & 1 \\ -1 & 0 \end{pmatrix}$ ,  $\Gamma_n \in \mathbb{R}^*$  is the vorticity (or vortex strength),  $\mathbf{r}_n \in \mathbb{R}^2$  is the position, of the  $n$ -th point vortex; and  $|\cdot|$  denotes the Euclidean norm in  $\mathbb{R}^2$ .

It is well known that, the  $N$ -vortex problem has self-similar collapsing solutions, that is, point vortices simultaneously collide with each other such that the relative shape remains constant; and the mechanism of vortex collapse plays an important role to understand fluid phenomena. For more detail please refer to [3, 11, 16] and references therein.

Following O’Neil [12], we will call a configuration stationary if it leads to a self-similar solution. In [12] it is shown that the only stationary configurations of vortices are equilibria, rigidly translating configurations, relative equilibria (uniformly rotating configurations) and collapse configurations. Certainly, collapse configurations lead to self-similar collapsing solutions.

In this paper, we are interested in the number of stationary configurations, especially, the number of collapse configurations, for given vorticities.

As everyone knows, all stationary configurations for two and three point vortices are known explicitly [7, 15, 11, 2, etc]. However, aside from special cases with certain symmetries [4], the only general work on stationary configurations, especially on relative equilibria and collapse configurations, is for four point vortices.

For the four-vortex problem, O’Neil [13] and Hampton and Moeckel [8] independently proved that for almost every choice of vorticities, there are finite equilibria, rigidly translating configurations and relative equilibria. In [16] it is shown that there are finitely many stationary configurations for every choice of vorticities, however, here finiteness on collapse configurations is only established for fixed collapse constants.

More specifically, in [16] we proved

**Theorem 1.1** *If all the vorticities of the four-vortex problem are nonzero, then there are finitely many stationary configurations for any given  $\Lambda \in \mathbb{C}^*$ .*

**Corollary 1.2** *If all the vorticities of the four-vortex problem are nonzero, then there are:*

- I. *exactly 2 equilibria when the necessary condition  $L = 0$  holds*
- II. *at most 6 rigidly translating configurations the necessary condition  $\Gamma = 0$  holds*
- III. *at most 12 collinear relative equilibria, more precisely,*
  - i. *at most 12 collinear relative equilibria when  $L \neq 0$*
  - ii. *at most 10 collinear relative equilibria when  $L = 0$*
  - iii. *at most 6 collinear relative equilibria when  $L \neq 0$  and  $\Gamma = 0$*
- IV. *at most 74 strictly planar relative equilibria, furthermore, at most 14 strictly planar relative equilibria when  $L \neq 0$  and  $\Gamma = 0$*
- V. *at most 130 collapse configurations for any given  $\Lambda \in \mathbb{C} \setminus \mathbb{R}$  when the necessary condition  $L = 0$  holds.*

Here please see Definition 2.2 and Definition 2.3 for the meaning of the collapse constant  $\Lambda$ . We remark that a configuration is called strictly planar if it is planar but not collinear, and planar configurations include collinear and strictly planar configurations.

The main purpose of the present study is to show that there are finitely many collapse configurations in the four-vortex problem, as a result, we have

**Theorem 1.3** *If all the vorticities of the four-vortex problem are nonzero, then there are finitely many stationary configurations.*

The result is an amazing fact. Recall that Synge [15] proved that the three-vortex problem has a continuum of collapse configurations. Therefore, it is generally believed that there are infinitely many collapse configurations in the  $N$ -vortex problem. Indeed, if one considers the parameter  $\Lambda$  in equations of collapse configurations (see (2.6), (2.11) or (3.15) below) as an unknown quantity, then the number of unknown quantities exceeds the number of equations and the system of equations is indefinite in form. As an example, we find a continuum of collapse configurations in the five-vortex problem.

The proof of Theorem 1.3 is based upon an extension of the elegant method of Albouy and Kaloshin for celestial mechanics [1] by absorbing some advantages of the method of BKK theory of Hampton and Moeckel [8]. The principle of the method is still to follow a possible continuum of collapse configurations in the complex domain and to study its possible singularities there. But we find that one can combine ideas of Albouy-Kaloshin and Hampton-Moeckel to do an analysis of the singularities with more subtlety than before. Roughly speaking, the method of Albouy and Kaloshin does not require any difficult computation, but it can only analyze leading coefficients of a polynomial system; on the other hand, the method of Hampton and Moeckel can analyze more coefficients of a polynomial system, but it requires difficult computations by employing Computer.

Here we still embed equations of collapse configurations into a polynomial system (see [16] and the following (3.15)), then a continuum of collapse configurations is excluded by an analysis of the singularities. Indeed, if the polynomial system has infinitely many solutions, then there are Puiseux series solutions. By analyzing leading coefficients of Puiseux series solutions, the original polynomial system is replaced by many simpler “reduced systems” for which one would like to show that the vorticities must satisfy some constraints. Roughly speaking, by showing these constraints on the vorticities are conflict with each other, one shows that the original polynomial system has finitely many solutions. By the way, if constraints on the vorticities obtained by analyzing leading coefficients of Puiseux series solutions are consistent with each other, one can further analyze second coefficients and so on to get more constraints on the vorticities for reducing to absurdity.

Once finiteness of the number of collapse configurations is proved, an explicit upper bound on the number of collapse configurations is obtained by a direct application of Bézout Theorems. However, such a bound is probably still far from sharp. Nevertheless, we also provide upper bounds in the following summary result:

**Corollary 1.4** *If all the vorticities of the four-vortex problem are nonzero, then, besides cases I, II, III and IV are same as that in Corollary 1.4, we have the following result to replace the case V in Corollary 1.4:*

- V. there are at most 98 collapse configurations when the necessary condition  $L = 0$  holds; more precisely,*
  - i. there are at most 108 central configurations when  $L = 0$*
  - ii. there are at most 98 collapse configurations, thus the number of  $\Lambda \in \mathbb{S}$  associated with collapse configurations is also no more than 98*

iii. there are at most 49 collapse configurations for every  $\Lambda \in \mathbb{S} \setminus \{\pm 1, \pm \mathbf{i}\}$ ; there are at most 98 collapse configurations for every  $\Lambda \in \{\pm \mathbf{i}\}$ .

The paper is structured as follows. In **Section 2**, we recall some notations and definitions given in [16]. In particular, following Hampton and Moeckel [8], we introduce Puiseux series solutions of a polynomial system. In **Section 3**, we discuss some tools to classify leading terms of Puiseux series solutions. In **Section 4** and **Section 5**, we study all possibilities of leading terms of Puiseux series solutions and reduce the problem to the seven diagrams in Figure 11 and in Figure 15; in particular, we get constraints on the vorticities corresponding to each of the seven diagrams. In **Section 6**, based upon the prior work, we prove the main result on finiteness. In **Section 7**, we investigate upper bounds on the number of collapse configurations. Finally, in **Section 8**, we conclude the paper by showing the existence of a continuum of collapse configurations in the five-vortex problem.

## 2 Preliminaries

In this section we recall some notations and definitions that will be needed later. For more detail please refer to [16].

### 2.1 Stationary configurations

First, let us consider vortex positions  $\mathbf{r}_n \in \mathbb{R}^2$  as complex numbers  $z_n \in \mathbb{C}$ , then (1.1) becomes  $\dot{z}_n = -\mathbf{i}V_n$ , where

$$V_n = \sum_{1 \leq j \leq N, j \neq n} \frac{\Gamma_j z_{jn}}{r_{jn}^2} = \sum_{j \neq n} \frac{\Gamma_j}{\bar{z}_{jn}}, \quad (2.2)$$

$z_{jn} = z_n - z_j$ ,  $r_{jn} = |z_{jn}| = \sqrt{z_{jn}\bar{z}_{jn}}$ ,  $\mathbf{i} = \sqrt{-1}$  and the overbar denotes complex conjugation.

Let  $\mathbb{C}^N = \{z = (z_1, \dots, z_N) : z_j \in \mathbb{C}, j = 1, \dots, N\}$  denote the space of configurations for  $N$  point vortex, and let  $\mathbb{C}^N \setminus \Delta$  denote the space of collision-free configurations.

**Definition 2.1** *The following quantities are defined:*

$$\begin{array}{ll} \text{Total vorticity} & \Gamma = \sum_{j=1}^N \Gamma_j \\ \text{Total vortex angular momentum} & L = \sum_{1 \leq j < k \leq N} \Gamma_j \Gamma_k \\ \text{Moment of vorticity} & M = \sum_{j=1}^N \Gamma_j z_j \\ \text{Angular impulse} & I = \sum_{j=1}^N \Gamma_j |z_j|^2 = \sum_{j=1}^N \Gamma_j z_j \bar{z}_j \end{array}$$

and

$$\Gamma I - M \bar{M} = \sum_{1 \leq j < k \leq N} \Gamma_j \Gamma_k z_{jk} \bar{z}_{jk} = \sum_{1 \leq j < k \leq N} \Gamma_j \Gamma_k r_{jk}^2 \triangleq S, \quad (2.3)$$

$$\Gamma^2 - 2L > 0. \quad (2.4)$$

**Definition 2.2** A configuration  $z \in \mathbb{C}^N \setminus \Delta$  is stationary if there exists a constant  $\Lambda \in \mathbb{C}$  such that

$$V_j - V_k = \Lambda(z_j - z_k), \quad 1 \leq j, k \leq N. \quad (2.5)$$

**Definition 2.3** i.  $z \in \mathbb{C}^N \setminus \Delta$  is an equilibrium if  $V_1 = \dots = V_N = 0$ .

ii.  $z \in \mathbb{C}^N \setminus \Delta$  is rigidly translating if  $V_1 = \dots = V_N = V$  for some  $V \in \mathbb{C}^*$ . (The vortices are said to move with common velocity  $V$ .)

iii.  $z \in \mathbb{C}^N \setminus \Delta$  is a relative equilibrium if there exist constants  $\lambda \in \mathbb{R}^*$ ,  $z_0 \in \mathbb{C}$  such that  $V_n = \lambda(z_n - z_0)$ ,  $1 \leq n \leq N$ .

iv.  $z \in \mathbb{C}^N \setminus \Delta$  is a collapse configuration if there exist constants  $\Lambda, z_0 \in \mathbb{C}$  with  $\text{Im}(\Lambda) \neq 0$  such that  $V_n = \Lambda(z_n - z_0)$ ,  $1 \leq n \leq N$ .

Where  $\mathbb{R}^* = \mathbb{R} \setminus \{0\}$ ,  $\mathbb{C}^* = \mathbb{C} \setminus \{0\}$ .

In [12], it is shown that the only stationary configurations of vortices are equilibria, rigidly translating configurations, relative equilibria (uniformly rotating configurations) and collapse configurations; in particular,  $L = 0$  is a necessary condition for the existence of equilibria, and  $\Gamma = 0$  is a necessary condition for the existence of configurations.

**Definition 2.4** A configuration  $z$  is equivalent to a configuration  $z'$  if for some  $a, b \in \mathbb{C}$  with  $b \neq 0$ ,  $z'_n = b(z_n + a)$ ,  $1 \leq n \leq N$ .

$z \in \mathbb{C}^N \setminus \Delta$  is a translation-normalized configuration if  $M = 0$ ;  $z \in \mathbb{C}^N \setminus \Delta$  is a rotation-normalized configuration if  $z_{12} \in \mathbb{R}$ . Fixing the scale of a configuration, we can give the definition of dilation-normalized configuration, however, we do not specify the scale here.

A configuration, which is translation-normalized, rotation-normalized and dilation-normalized, is called a **normalized configuration**.

**Definition 2.5** Relative equilibria and collapse configurations are both called **central configurations**.

Recall that equations of relative equilibria and collapse configurations can be unified into the following form

$$\Lambda z_n = V_n, \quad 1 \leq n \leq N, \quad (2.6)$$

and solutions of equations (2.6) satisfy

$$M = 0, \quad (2.7)$$

$$\Lambda I = L. \quad (2.8)$$

Following Albouy and Kaloshin [1] we introduce

**Definition 2.6** A real normalized central configuration of the planar  $N$ -vortex problem is a solution of (2.6) satisfying  $z_{12} \in \mathbb{R}$  and  $|\Lambda| = 1$ .

Note that real normalized central configurations come in a pair, that is, central configurations is determined up to a common factor  $\pm 1$  by normalizing here. Thus we count the total central configurations up to a common factor  $\pm 1$  below.

**Proposition 2.1** *Collapse configurations satisfy  $\Gamma \neq 0$  and*

$$S = I = L = 0. \quad (2.9)$$

*For relative equilibria we have*

$$S = 0 \iff \begin{cases} \Gamma \neq 0 \\ I = L = 0 \end{cases} \quad \text{or} \quad \begin{cases} \Gamma = 0 \\ I \neq 0, L \neq 0 \end{cases}$$

In this paper we mainly study collapse configurations. Thus we assume that the total vortex angular momentum is trivial in the following, i.e., (2.1) holds.

## 2.2 Complex central configurations

We embed (2.6) into

$$\begin{aligned} \Lambda z_n &= \sum_{j \neq n} \frac{\Gamma_j}{w_{jn}}, & 1 \leq n \leq N, \\ \bar{\Lambda} w_n &= \sum_{j \neq n} \frac{\Gamma_j}{z_{jn}}, & 1 \leq n \leq N, \end{aligned} \quad (2.10)$$

where  $z_{jn} = z_n - z_j$  and  $w_{jn} = w_n - w_j$ . The condition  $z_{12} \in \mathbb{R}$  we proposed to remove the rotation freedom becomes  $z_{12} = w_{12}$ .

Note that  $I, S$  become

$$I = \sum_{j=1}^N \Gamma_j z_j w_j, \quad S = \sum_{1 \leq j < k \leq N} \Gamma_j \Gamma_k r_{jk}^2 = \sum_{1 \leq j < k \leq N} \Gamma_j \Gamma_k z_{jk} w_{jk}.$$

To the variables  $z_n, w_n \in \mathbb{C}$  we add the variables  $Z_{jk}, W_{jk} \in \mathbb{C}$  ( $1 \leq j < k \leq N$ ) such that  $Z_{jk} = \frac{1}{\Lambda w_{jk}}, W_{jk} = \frac{\Lambda}{z_{jk}}$ . For  $1 \leq k < j \leq N$  we set  $Z_{jk} = -Z_{kj}, W_{jk} = -W_{kj}$ . Then equations (2.6) together with the condition  $z_{12} \in \mathbb{R}$  and  $|\Lambda| = 1$  becomes

$$\begin{aligned} z_n &= \sum_{j \neq n} \Gamma_j Z_{jn}, & 1 \leq n \leq N, \\ w_n &= \sum_{j \neq n} \Gamma_j W_{jn}, & 1 \leq n \leq N, \\ \Lambda Z_{jk} w_{jk} &= 1, & 1 \leq j < k \leq N, \\ W_{jk} z_{jk} &= \Lambda, & 1 \leq j < k \leq N, \\ z_{jk} &= z_k - z_j, \quad w_{jk} = w_k - w_j, & 1 \leq j, k \leq N, \\ Z_{jk} &= -Z_{kj}, \quad W_{jk} = -W_{kj}, & 1 \leq k < j \leq N, \\ z_{12} &= w_{12}. \end{aligned} \quad (2.11)$$

This is a polynomial system in the variables  $\Omega = (\mathcal{Z}, \mathcal{W}) \in (\mathbb{C}^N \times \mathbb{C}^{N(N-1)/2})^2$ , here

$$\begin{aligned} \mathcal{Z} &= (z_1, z_2, \dots, z_N, Z_{12}, Z_{13}, \dots, Z_{(N-1)N}), \\ \mathcal{W} &= (w_1, w_2, \dots, w_N, W_{12}, W_{13}, \dots, W_{(N-1)N}). \end{aligned}$$

It is easy to see that a real normalized central configuration of (2.6) is a solution  $\mathcal{Q} = (\mathcal{Z}, \mathcal{W})$  of (2.11) such that  $z_n = \bar{w}_n$  and vice versa.

Following Albouy and Kaloshin [1] we introduce

**Definition 2.7 (Normalized central configuration)** *A normalized central configuration is a solution  $\mathcal{Q} = (\mathcal{Z}, \mathcal{W})$  of (2.11). A real normalized central configuration is a normalized central configuration such that  $z_n = \bar{w}_n$  for any  $n = 1, 2, \dots, N$ .*

*A (real) normalized relative equilibrium (resp. collapse configuration) is (real) a normalized central configuration with  $\Lambda = \pm 1$  (resp.  $\Lambda \in \mathbb{S} \setminus \{\pm 1\}$ ).*

*Where  $\mathbb{S}$  is the unit circle in  $\mathbb{C}$ .*

Definition 2.7 of a real normalized central configuration coincides with Definition 2.6.

Note that solutions  $\mathcal{Q} = (\mathcal{Z}, \mathcal{W})$  of (2.11) come in a pair:  $(-\mathcal{Z}, -\mathcal{W}) \mapsto (\mathcal{Z}, \mathcal{W})$  sends solution on solution, that is, a solution of (2.11) is determined up to a common factor  $\pm 1$ .

## 2.3 Elimination theory

Recall that, a closed algebraic subset of the affine space  $\mathbb{C}^m$  is a set of common zeroes of a system of polynomials on  $\mathbb{C}^m$ . The polynomial system (2.11) defines a closed algebraic subset. For the planar four-vortex problem, we will prove that this subset is finite, then the number of real normalized central configurations is finite. To distinguish the two possibilities, finitely many or infinitely many points, we will only use the following results from elimination theory.

**Lemma 2.1** ([1]) *Let  $\mathcal{X}$  be a closed algebraic subset of  $\mathbb{C}^m$  and  $f : \mathbb{C}^m \rightarrow \mathbb{C}$  be a polynomial. Either the image  $f(\mathcal{X}) \subset \mathbb{C}$  is a finite set, or it is the complement of a finite set. In the second case one says that  $f$  is dominating.*

In particular, we remark that the polynomial functions  $I$  and  $S$ , on the closed algebraic subset  $\mathcal{A} \subset (\mathbb{C}^N \times \mathbb{C}^{N(N-1)/2})^2$  defined by the system (2.11), are two real constants.

**Lemma 2.2** ([9]) *Suppose that a system of  $n$  polynomial equations  $f_k$  defines an infinite variety  $\mathcal{X} \subset \mathbb{C}^m$ . Then there is a nonzero rational vector  $\alpha = (\alpha_1, \dots, \alpha_m)$ ,  $m$  nonzero numbers  $a_j$ , and Puiseux series  $x_j(t) = a_j t^{\alpha_j} + \dots$ ,  $j = 1, \dots, m$ , convergent in some punctured neighborhood  $U$  of  $t = 0$ , such that  $f_k(x_1(t), \dots, x_m(t)) = 0$  in  $U$ ,  $k = 1, \dots, n$ . Moreover, let  $g : \mathbb{C}^m \rightarrow \mathbb{C}$  be a polynomial, if  $g$  is dominating, there exists such a series solution with  $g(t) = t$  and another with  $g(t) = t^{-1}$ ; for example, if the projection from  $\mathcal{X}$  onto the  $x_i$ -axis is dominant, there exists such a series solution with  $x_i(t) = t$  and another with  $x_i(t) = t^{-1}$ .*

Lemma 2.2 is a slight variation of Proposition 1 in [9]. Since the proof of Lemma 2.2 is quite similar to that given by Hampton and Moeckel in [9], no proof will be given here.

## 2.4 Bézout Theorem

After finiteness of the number of central configurations is established, we mainly make use of a refined version of Bézout Theorem to discuss upper bounds of the number of real normalized central configurations.

**Lemma 2.3** ([14]) *Let  $\mathcal{V}_1, \dots, \mathcal{V}_m$  be pure dimensional subvarieties of  $\mathbb{P}^N$ . Let  $\mathcal{U}_1, \dots, \mathcal{U}_n$  be the irreducible components of  $\mathcal{X} \triangleq \mathcal{V}_1 \cap \dots \cap \mathcal{V}_m$ . Then*

$$\sum_{j=1}^n l(\mathcal{X}; \mathcal{U}_j) \deg(\mathcal{U}_j) \leq \prod_{j=1}^m \deg(\mathcal{V}_j), \quad (2.12)$$

where  $l(\mathcal{X}; \mathcal{U}_j)$  is the length of well-defined primary ideals, i.e., the multiplicity of  $\mathcal{X}$  along  $\mathcal{U}_j$ .

**Definition 2.8** (See [5]) *The multiplicity  $l(\mathcal{X}; P)$  of  $\mathcal{X}$  at a point  $P \in \mathcal{X}$  is the degree of the projectivized tangent cone  $\mathbb{T}C_P \mathcal{X}$ . The multiplicity  $l(\mathcal{X}; \mathcal{U})$  of a scheme  $\mathcal{X}$  along an irreducible component  $\mathcal{U}$ , is equal to the multiplicity of  $\mathcal{X}$  at a general point of  $\mathcal{U}$ .*

**Lemma 2.4** ([6]) *Let  $\mathcal{V}_1, \dots, \mathcal{V}_m$  be pure-dimensional subschemes of  $\mathbb{P}^N$ , with*

$$\sum_{j=1}^m \dim(\mathcal{V}_j) = (m-1)N.$$

Assume  $P$  is an isolated point of  $\mathcal{X} \triangleq \mathcal{V}_1 \cap \dots \cap \mathcal{V}_m$ . Then

$$l(\mathcal{X}; P) \geq \prod_{j=1}^m l(\mathcal{V}_j; \mathcal{U}) + \sum_{j=1}^n \deg(\mathcal{U}_j), \quad (2.13)$$

where  $\mathcal{U}_1, \dots, \mathcal{U}_n$  are the irreducible components of  $\mathbb{T}C_P \mathcal{V}_1 \cap \dots \cap \mathbb{T}C_P \mathcal{V}_m$ . In particular,

$$l(\mathcal{X}; P) \geq \prod_{j=1}^m l(\mathcal{V}_j; \mathcal{U}) \quad (2.14)$$

with equality if and only if  $\mathbb{T}C_P \mathcal{V}_1 \cap \dots \cap \mathbb{T}C_P \mathcal{V}_m = \emptyset$ .

## 3 Puiseux series solutions and colored diagram

Consider the following equations for variables  $\Lambda, z_n, w_n, Z_{jk}, W_{jk} \in \mathbb{C}$ ,  $n = 1, \dots, N$ ,  $1 \leq j < k \leq N$ :

$$\begin{aligned} z_n &= \sum_{j \neq n} \Gamma_j Z_{jn}, & 1 \leq n \leq N, \\ w_n &= \sum_{j \neq n} \Gamma_j W_{jn}, & 1 \leq n \leq N, \\ \Lambda Z_{jk} w_{jk} &= 1, & 1 \leq j < k \leq N, \\ W_{jk} z_{jk} &= \Lambda, & 1 \leq j < k \leq N, \\ z_{jk} &= z_k - z_j, & w_{jk} &= w_k - w_j, & 1 \leq j, k \leq N, \\ Z_{jk} &= -Z_{kj}, & W_{jk} &= -W_{kj}, & 1 \leq k < j \leq N, \\ z_{12} &= w_{12}. \end{aligned} \quad (3.15)$$

It is easy to see that, if there are infinitely many  $\Lambda \in \mathbb{S}$  such that the equations (2.11) have a solution, then the system of equations (3.15) defines an infinite variety  $\mathcal{X} \subset \mathbb{C} \times (\mathbb{C}^N \times \mathbb{C}^{N(N-1)/2})^2$ , and the projection from  $\mathcal{X}$  onto the  $\Lambda$ -axis is dominant. By Lemma 2.2, it follows that there is a nonzero rational vector

$$(\alpha, \beta, \gamma) = (\alpha_1, \dots, \alpha_N, \alpha_{12}, \dots, \alpha_{(N-1)N}, \beta_1, \dots, \beta_N, \beta_{12}, \dots, \beta_{(N-1)N}, \gamma),$$

a vector

$$(a, b, c) = (a_1, \dots, a_N, A_{12}, \dots, A_{(N-1)N}, b_1, \dots, b_N, B_{12}, \dots, B_{(N-1)N}, c) \in \mathbb{C}^{*N(N+1)+1},$$

and Puiseux series

$$\begin{aligned} z_n(t) &= a_n t^{\alpha_n} + \dots, & w_n(t) &= b_n t^{\beta_n} + \dots, & n &= 1, \dots, N \\ Z_{jk}(t) &= \frac{1}{\Lambda(t)z_{jk}(t)} = A_{jk} t^{\alpha_{jk}} + \dots, & W_{jk}(t) &= \frac{\Lambda(t)}{w_{jk}(t)} = B_{jk} t^{\beta_{jk}} + \dots, & 1 \leq j < k \leq N \\ \Lambda(t) &= ct^\gamma + \dots, \end{aligned} \tag{3.16}$$

convergent in some punctured neighborhood  $U$  of  $t = 0$ , such that the system of equations (3.15) holds for any  $t \in U$ .

Note that, by the projection from  $\mathcal{X}$  onto the  $\Lambda$ -axis is dominant, there are Puiseux series as (3.16) with  $\Lambda(t) = t$  or with  $\Lambda(t) = t^{-1}$ .

Following Hampton and Moeckel [8], a vector of nonzero Puiseux series

$$\mathcal{Q}(t) = (\mathcal{Z}(t), \mathcal{W}(t))$$

as (3.16) will be said to have order  $(\alpha, \beta)$ . Here recall that,

$$\begin{aligned} \mathcal{Z} &= (z_1, z_2, \dots, z_N, Z_{12}, Z_{13}, \dots, Z_{(N-1)N}), \\ \mathcal{W} &= (w_1, w_2, \dots, w_N, W_{12}, W_{13}, \dots, W_{(N-1)N}). \end{aligned}$$

Therefore, to prove the finiteness of  $\Lambda \in \mathbb{S}$ , it suffices to show that for every nonzero rational vector  $(\alpha, \beta)$  there is no Puiseux series solution of order  $(\alpha, \beta)$ . To this end, one can apply the method of BKK theory by Hampton and Moeckel [8]. However, we will not utilize this method in this paper, because it has a large amount of calculation. Instead, we will utilize a method similar as in [16] to show that Puiseux series solutions of a given order do not exist.

### 3.1 Notations and definitions

**Definition 3.1 (Notations on Puiseux series)** *For a given Puiseux series  $x(t) = at^q + \dots$  with the leading term  $at^q$ , let  $q = d(x(t))$  denote the degree of  $x(t)$ , and set*

$$at^q =: L(x(t)).$$

*For a given vector of nonzero Puiseux series*

$$\mathcal{Q}(t) = (\mathcal{Z}(t), \mathcal{W}(t))$$

of order  $(\alpha, \beta)$  as (3.16), set

$$|\mathcal{Z}(t)| = |\alpha| := \min\{\alpha_1, \dots, \alpha_N, \alpha_{12}, \dots, \alpha_{(N-1)N}\},$$

$$|\mathcal{W}(t)| = |\beta| := \min\{\beta_1, \dots, \beta_N, \beta_{12}, \dots, \beta_{(N-1)N}\},$$

$$|\mathcal{Q}(t)| := \min\{|\mathcal{Z}(t)|, |\mathcal{W}(t)|\},$$

which denote the degrees of  $\mathcal{Z}(t)$ ,  $\mathcal{W}(t)$  and  $\mathcal{Q}(t)$ , respectively.

**Definition 3.2 (Notations of asymptotic estimates)** Given two Puiseux series  $x, y$ , we have:

$x \sim y$  means  $L(x) = L(y)$ ;

$x \prec y$  means  $d(x) > d(y)$ ;

$x \preceq y$  means  $d(x) \geq d(y)$ ;

$x \approx y$  means  $d(x) = d(y)$ .

**Definition 3.3 (Strokes and circles.)** We pick a Puiseux series  $\mathcal{Q}$ . We write the indices of the bodies in a figure and use two colors for edges and vertices.

The first color, the  $z$ -color, is used to mark the minimal degree components of

$$\mathcal{Z} = (z_1, z_2, \dots, z_N, Z_{12}, Z_{13}, \dots, Z_{(N-1)N}).$$

They correspond to the components that whose degrees are equal to  $|\mathcal{Z}|$ . We draw a circle around the name of vertex  $\mathbf{n}$  if the term  $z_n$  is of minimal degree among all the components of  $\mathcal{Z}$ . We draw a stroke between the names  $\mathbf{j}$  and  $\mathbf{k}$  if the term  $Z_{jk}$  is of minimal degree among all the components of  $\mathcal{Z}$ .

Similar as in [16], we have the following rules mainly concern  $z$ -diagram, but they apply as well to the  $w$ -diagram.

**Rule I** There is something at each end of any  $z$ -stroke: another  $z$ -stroke or/and a  $z$ -circle drawn around the name of the vertex. A  $z$ -circle cannot be isolated; there must be a  $z$ -stroke emanating from it. There is at least one  $z$ -stroke in the  $z$ -diagram.

**Definition 3.4 ( $z$ -close)** Consider a Puiseux series. We say that bodies  $\mathbf{k}$  and  $\mathbf{l}$  are close in  $z$ -coordinate, or  $z$ -close, or that  $z_k$  and  $z_l$  are close, if  $z_{kl} \prec \mathcal{Z}$ .

**Rule II** If bodies  $\mathbf{k}$  and  $\mathbf{l}$  are  $z$ -close, they are both  $z$ -circled or both not  $z$ -circled.

**Definition 3.5 (Isolated component)** An isolated component of the  $z$ -diagram is a subset of vertices such that no  $z$ -stroke is joining a vertex of this subset to a vertex of the complement.

**Rule III** The moment of vorticity of a set of bodies forming an isolated component of the  $z$ -diagram is  $z$ -close to the origin.

**Rule IV** Consider the  $z$ -diagram or an isolated component of it. If there is a  $z$ -circled vertex, there is another one. The  $z$ -circled vertices can all be  $z$ -close together only if the total vorticity of these vertices is zero.

**Definition 3.6 (Maximal  $z$ -stroke)** Consider a  $z$ -stroke from vertex  $\mathbf{k}$  to vertex  $\mathbf{l}$ . We say it is a maximal  $z$ -stroke if  $\mathbf{k}$  and  $\mathbf{l}$  are not  $z$ -close.

**Rule V** There is at least one  $z$ -circle at certain end of any maximal  $z$ -stroke. As a result, if an isolated component of the  $z$ -diagram has no  $z$ -circled vertex, then it has no maximal  $z$ -stroke.

On the same diagram we also draw  $w$ -strokes and  $w$ -circles. Graphically we use another color. The previous rules and definitions apply to  $w$ -strokes and  $w$ -circles. What we will call simply the diagram is the superposition of the  $z$ -diagram and the  $w$ -diagram. We will, for example, adapt Definition 3.5 of an isolated component: a subset of bodies forms an isolated component of the diagram if and only if it forms an isolated component of the  $z$ -diagram and an isolated component of the  $w$ -diagram.

**Definition 3.7 (Edges and strokes)** There is an edge between vertex  $\mathbf{k}$  and vertex  $\mathbf{l}$  if there is either a  $z$ -stroke, or a  $w$ -stroke, or both. There are three types of edges,  $z$ -edges,  $w$ -edges and  $zw$ -edges, and only two types of strokes, represented with two different colors.



Figure 1: A  $z$ -stroke, a  $z$ -stroke plus a  $w$ -stroke, a  $w$ -stroke, forming respectively a  $z$ -edge, a  $zw$ -edge, a  $w$ -edge.

### 3.2 New normalization. Main estimates.

One does not change a central configuration by multiplying the  $z$  coordinates by  $t^p$  and the  $w$  coordinates by  $t^{-p}$  for any  $p \in \mathbb{Q}$ . Our diagram is invariant by such an operation, as it considers the  $z$ -coordinates and the  $w$ -coordinates separately.

We used the normalization  $z_{12} = w_{12}$  in the previous considerations. In the following we will normalize instead with  $|\mathcal{Z}| = |\mathcal{W}|$ . We start with a central configuration normalized with the condition  $z_{12} = w_{12}$ , then multiply the  $z$ -coordinates by  $t^p$ , the  $w$ -coordinates by  $t^{-p}$ , in such a way that  $|\mathcal{Z}| = |\mathcal{W}|$ .

Set  $|\mathcal{Z}| = |\mathcal{W}| = q$ , here  $q \in \mathbb{Q}$ . Similar as in [16], we have

**Proposition 3.1 (Estimate 2)** For any  $(k, l)$ ,  $1 \leq k < l \leq N$ , we have  $t^{\gamma-q} \preceq z_{kl} \preceq t^q$  and  $t^{-\gamma-q} \preceq w_{kl} \preceq t^q$ ; thus  $q \leq -\frac{|\gamma|}{2}$ .

There is a  $z$ -stroke between  $\mathbf{k}$  and  $\mathbf{l}$  if and only if  $w_{kl} \approx t^{-\gamma-q}$ ; there is a  $w$ -stroke between  $\mathbf{k}$  and  $\mathbf{l}$  if and only if  $z_{kl} \approx t^{\gamma-q}$ .

There is a maximal  $z$ -stroke between  $\mathbf{k}$  and  $\mathbf{l}$  if and only if  $z_{kl} \approx t^q, w_{kl} \approx t^{-\gamma-q}$ ; there is a maximal  $w$ -stroke between  $\mathbf{k}$  and  $\mathbf{l}$  if and only if  $z_{kl} \approx t^{\gamma-q}, w_{kl} \approx t^q$ .

There is a  $z$ -edge between  $\mathbf{k}$  and  $\mathbf{l}$  if and only if  $z_{kl} \succ t^{\gamma-q}, w_{kl} \approx t^{-\gamma-q}$ ; there is a  $w$ -edge between  $\mathbf{k}$  and  $\mathbf{l}$  if and only if  $z_{kl} \approx t^{\gamma-q}, w_{kl} \succ t^{-\gamma-q}$ .

There is a maximal  $z$ -edge between  $\mathbf{k}$  and  $\mathbf{l}$  if and only if  $z_{kl} \approx t^q, w_{kl} \approx t^{-\gamma-q}$ ; there is a maximal  $w$ -edge between  $\mathbf{k}$  and  $\mathbf{l}$  if and only if  $z_{kl} \approx t^{\gamma-q}, w_{kl} \approx t^q$ .

There is a  $zw$ -edge between  $\mathbf{k}$  and  $\mathbf{l}$  if and only if  $z_{kl} \approx t^{\gamma-q}, w_{kl} \approx t^{-\gamma-q}$ .

**Rule VI** If there are two consecutive  $z$ -stroke, there is a third  $z$ -stroke closing the triangle.

Similar to [16], we classify all possible diagrams by these rules of coloring diagrams in the following two sections. We divide discussions into two cases according to  $q < -\frac{|\gamma|}{2}$  or  $q = -\frac{|\gamma|}{2}$ . Note that we only consider the case that  $q < 0$  below, since we will only face this case when we practically construct Puiseux series.

## 4 Possible diagrams in the case $q < -|\gamma|/2$

In this section, we consider the case that  $q < -\frac{|\gamma|}{2}$ . Then it is easy to see that, by estimates in Proposition 3.1, we have

**Remark 4.1** The strokes in a  $zw$ -edge are not maximal. A maximal  $z$ -stroke (resp.  $w$ -stroke) is exactly a maximal  $z$ -edge (resp.  $w$ -edge). In particular, if vertices  $\mathbf{k}$  and  $\mathbf{l}$  form a  $z$ -stroke (resp.  $w$ -stroke), then they are  $w$ -close (resp.  $z$ -close).

Consequently, we remark that the rules for coloring diagrams in this section are exactly same as that in Section 3 in [16].

### 4.1 Possible diagrams

Based upon the results in previous sections, it is easy to see that the only possible diagrams are exactly same as that in Subsection 4.1 in [16], i.e., Figures 2–10 in [16]. For convenience, these Figures are presented below.

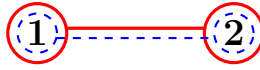
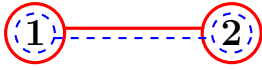
Proposition 4.1 in Subsection 4.2 in [16] may be wrong generally, here we propose the following proposition to replace Proposition 4.1 in [16].

**Proposition 4.1** Suppose a diagram has two  $z$ -circled vertices (say  $\mathbf{1}$  and  $\mathbf{2}$ ) without other  $z$ -circled vertices. If vertices  $\mathbf{1}$  and  $\mathbf{2}$  form a  $z$ -stroke, then  $\Gamma_1 + \Gamma_2 \neq 0$ .

**Proof.**



Figure 2



4

3



Figure 3

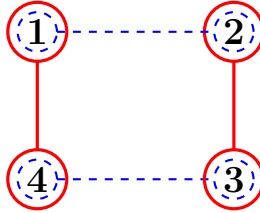


Figure 4

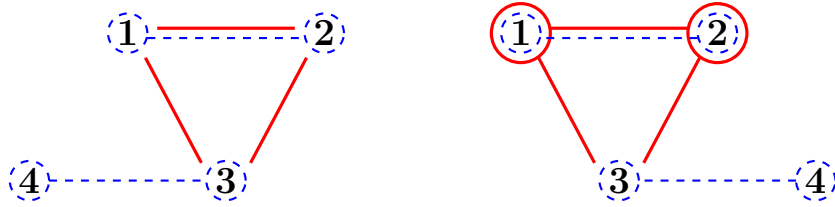


Figure 5

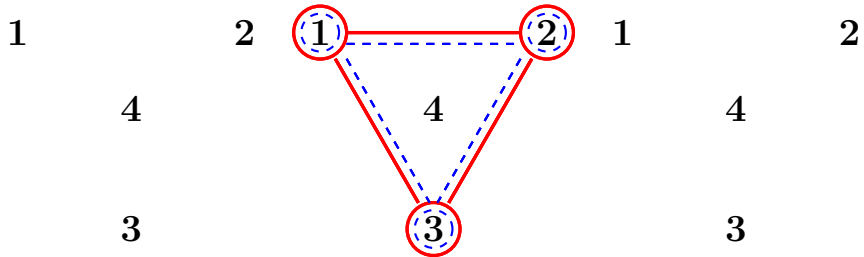


Figure 6

Without loss of generality, assume that

$$z_1 \sim -\Gamma_2 at^a, \quad z_2 \sim \Gamma_1 at^a, \quad w_{12} \sim \frac{1}{ac} t^{-\gamma-a},$$

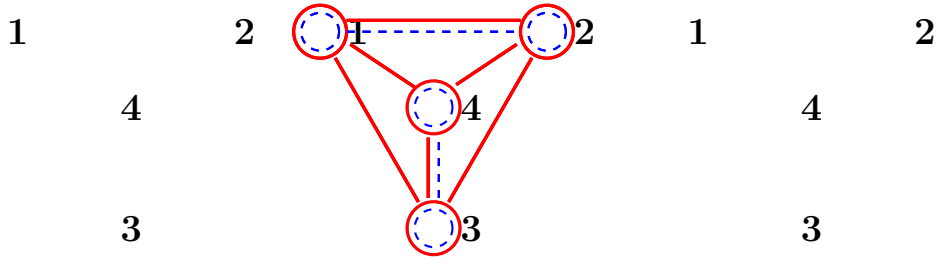


Figure 7

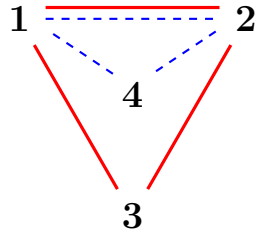


Figure 8

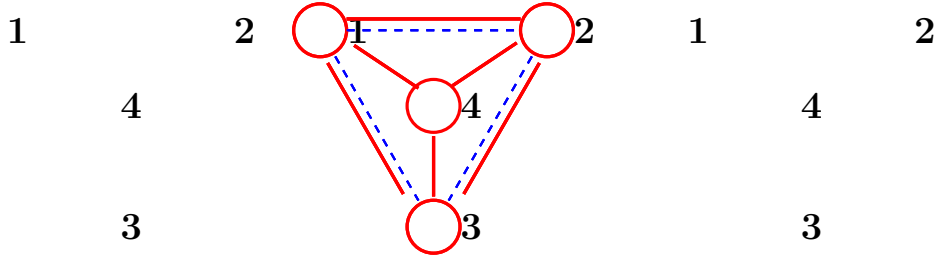


Figure 9

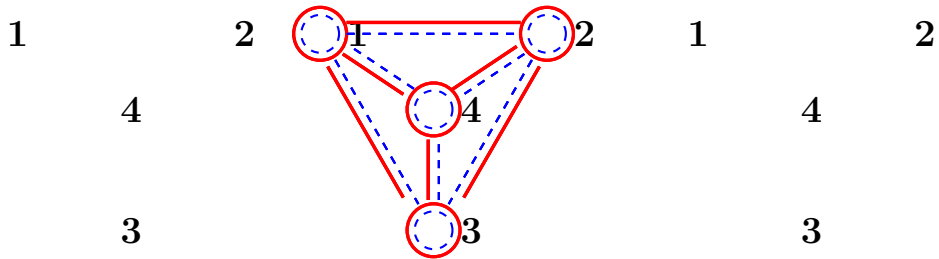


Figure 10

here recall that  $\Lambda \sim ct^\gamma$ .

If  $\Gamma_1 + \Gamma_2 = 0$ , by  $L = 0$ , it is easy to see that  $\sum_{j>2} \Gamma_j \neq 0$ .

By

$$w_{12} = (\Gamma_1 + \Gamma_2)W_{12} + \sum_{j>2} \Gamma_j(W_{j2} - W_{j1}),$$

it follows that

$$\frac{1}{ac}t^{-\gamma-q} \sim w_{12} = -\sum_{j>2} \frac{\Gamma_j \Lambda z_{12}}{z_{1j} z_{2j}} \asymp -\frac{\sum_{j>2} \Gamma_j c t^\gamma z_{12}}{(\Gamma_1 a t^q)^2} \prec -\frac{\sum_{j>2} \Gamma_j c t^\gamma t^q}{(\Gamma_1 a t^q)^2}.$$

Then it is easy to see that

$$\gamma < 0, \quad z_{12} \sim \frac{a \Gamma_1^2}{c^2 \sum_{j>2} \Gamma_j} t^{q-2\gamma}.$$

By

$$z_{12} = (\Gamma_1 + \Gamma_2) Z_{12} + \sum_{j>2} \Gamma_j (Z_{j2} - Z_{j1}),$$

it follows that

$$\frac{\Lambda z_{12}}{w_{12}} = -\sum_{j>2} \frac{\Gamma_j}{w_{1j} w_{2j}}.$$

However, we have

$$\frac{\Lambda z_{12}}{w_{12}} \approx t^{2q} \succ t^{-2q} \succeq -\sum_{j>2} \frac{\Gamma_j}{w_{1j} w_{2j}},$$

this leads to a contradiction.

As a result,  $\Gamma_1 + \Gamma_2 \neq 0$  holds. □

On the other hand, it is noteworthy that Propositions 4.2, 4.3 and 4.4 in Subsection 4.2 in [16] are still correct. For convenience, these Figures are presented below. Their proofs are similar as that in [16], proofs will be omitted.

**Proposition 4.2** *Suppose a diagram has an isolated  $z$ -stroke, then vertices of it are both  $z$ -circled; if the two vertices are  $z$ -close (for example, provided the two vertices are connected by  $w$ -stroke), then the total vorticity of them is zero.*

**Proposition 4.3** *Suppose a diagram has an isolated  $z$ -color triangle, and none of vertices (say **1,2,3**) of it are  $z$ -circled, then  $\frac{1}{\Gamma_1} + \frac{1}{\Gamma_2} + \frac{1}{\Gamma_3} = 0$  or  $\Gamma_1 \Gamma_2 + \Gamma_2 \Gamma_3 + \Gamma_3 \Gamma_1 = 0$ .*

**Proposition 4.4** *Suppose a fully  $z$ -stroked sub-diagram with four vertices exists in isolation in a diagram, and none of vertices (say **1,2,3,4**) of it are  $z$ -circled, then*

$$L_{1234} = \Gamma_1 \Gamma_2 + \Gamma_2 \Gamma_3 + \Gamma_3 \Gamma_1 + \Gamma_4 (\Gamma_1 + \Gamma_2 + \Gamma_3) = 0. \quad (4.17)$$

By these Propositions, an argument similar to the one used in Subsection 4.2 in [16] shows that problematic diagrams also consist of the list in Figure 11 in [16]. Moreover, since we are focusing on four-vortex collapse configurations, and we assume that (2.1) holds,  $L = \sum_{1 \leq j < k \leq 4} \Gamma_j \Gamma_k = 0$  is a necessary condition, one can further exclude the diagrams in Figure 11 in [16].

## 4.2 Exclusion of diagrams

Now, for the sake of completeness, we further exclude diagrams in Figures 2–10 above by a case-by-case analysis.

### Figure 3:

For diagrams in Figure 3, by Proposition 4.2, it is easy to see that  $\Gamma_1 + \Gamma_2 = 0$  and the third diagram is impossible. Moreover, by Proposition 4.1, it follows that  $\Gamma_1 + \Gamma_2 \neq 0$  for the first two diagrams, this leads to a contradiction. As a result, diagrams in Figure 3 are impossible.

### Figure 5:

For the first diagram in Figure 5, by Proposition 4.3, it is easy to see that  $\frac{1}{\Gamma_1} + \frac{1}{\Gamma_2} + \frac{1}{\Gamma_3} = 0$ , therefore, the first diagram is impossible. For the second diagram in Figure 5, by Proposition 4.2, it follows that  $\Gamma_1 + \Gamma_2 = 0$ . However, by Proposition 4.1, it follows that  $\Gamma_1 + \Gamma_2 \neq 0$ . This leads to a contradiction. As a result, diagrams in Figure 5 are impossible.

### Figure 6:

For diagrams in Figure 6, it is easy to see that vorticities satisfy  $\frac{1}{\Gamma_1} + \frac{1}{\Gamma_2} + \frac{1}{\Gamma_3} = 0$  or  $\Gamma_1 + \Gamma_2 + \Gamma_3 = 0$ , but this is in conflict with  $L = 0$ . As a result, diagrams in Figure 6 are impossible.

### Figure 7:

For diagrams in Figure 7, it is easy to see that vorticities satisfy  $\Gamma_1 + \Gamma_2 = 0$  and  $\Gamma_3 + \Gamma_4 = 0$ , but these relations are in conflict with  $L = 0$ . As a result, diagrams in Figure 7 are impossible.

### Figure 8:

For the diagram in Figure 8, it is easy to see that vorticities satisfy  $\frac{1}{\Gamma_1} + \frac{1}{\Gamma_2} + \frac{1}{\Gamma_3} = 0$  and  $\frac{1}{\Gamma_1} + \frac{1}{\Gamma_2} + \frac{1}{\Gamma_4} = 0$ , but these relations are in conflict with  $L = 0$ . As a result, diagrams in Figure 8 are impossible.

### Figure 9:

For diagrams in Figure 9, it is easy to see that vorticities satisfy  $\frac{1}{\Gamma_1} + \frac{1}{\Gamma_2} + \frac{1}{\Gamma_3} = 0$ , but the relation is in conflict with  $L = 0$ . As a result, diagrams in Figure 9 are impossible.

### Figure 10:

For the last two diagrams in Figure 10, it is easy to see that vorticities satisfy  $\Gamma_1 + \Gamma_2 + \Gamma_3 + \Gamma_4 = 0$ , but this is in conflict with  $L = 0$ . As a result, the last two diagrams in Figure 10 are impossible.

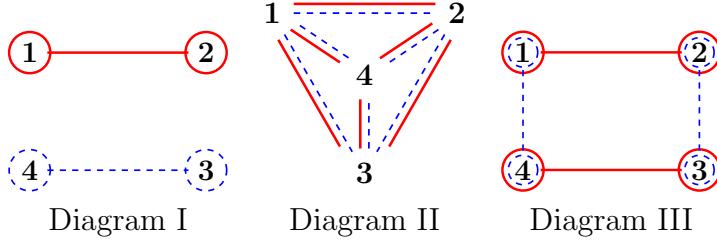


Figure 11: Problematic diagrams for  $q < -|\gamma|/2$

In conclusion, we have derived a list of problematic diagrams consisting of Diagram I, Diagram II and Diagram III in Figure 11. By the way, these diagrams are same as the first three diagrams in Figure 11 in [16].

### 4.3 Problematic diagrams

In general, we could not eliminate Diagram I, Diagram II or Diagram III. In this subsection we obtain constraints on the vorticities corresponding to each of these three diagrams.

#### 4.3.1 Diagram I

For the Diagram I, assume that

$$\begin{aligned} z_1 &\sim -\Gamma_2 at^q, & z_2 &\sim \Gamma_1 at^q, & w_{12} &\sim \frac{1}{ac} t^{-\gamma-q}, \\ w_3 &\sim -\Gamma_4 bt^q, & w_4 &\sim \Gamma_3 bt^q, & z_{34} &\sim \frac{c}{b} t^{\gamma-q}. \end{aligned}$$

First, by Proposition 4.1, it follows that

$$\Gamma_1 + \Gamma_2 \neq 0 \text{ and } \Gamma_3 + \Gamma_4 \neq 0.$$

Then, by

$$w_{12} = (\Gamma_1 + \Gamma_2)W_{12} + \Gamma_3(W_{32} - W_{31}) + \Gamma_4(W_{42} - W_{41})$$

and

$$z_{34} = (\Gamma_3 + \Gamma_4)Z_{34} + \Gamma_1(Z_{14} - Z_{13}) + \Gamma_2(Z_{24} - Z_{23}),$$

it follows that

$$\gamma = 0$$

and

$$\begin{aligned} \frac{1}{c^2} &= 1 + (\Gamma_3 + \Gamma_4)\left(\frac{1}{\Gamma_1} + \frac{1}{\Gamma_2}\right), \\ c^2 &= 1 + (\Gamma_1 + \Gamma_2)\left(\frac{1}{\Gamma_3} + \frac{1}{\Gamma_4}\right), \end{aligned}$$

or

$$c^2 = -\frac{\Gamma_1 \Gamma_2}{\Gamma_3 \Gamma_4}.$$

Note that, when Diagram I is possible, we have

$$r_{12} \approx r_{34} \approx t^0, \quad r_{13} \approx r_{14} \approx r_{23} \approx r_{24} \approx t^q, \quad (4.18)$$

in particular,

$$\frac{r_{ij}}{r_{kl}} \approx t^0, \quad (4.19)$$

where  $(ijkl)$  is any permutation of  $\{1, 2, 3, 4\}$ , i.e.,  $\{i, j, k, l\} = \{1, 2, 3, 4\}$ .

To summarize, the following relations on the four vorticities should be satisfied if Diagram I is possible by choosing a Puiseux series:

$$\begin{aligned} r_{12}^2 &\sim \frac{\Gamma_1 + \Gamma_2}{c} t^0, & r_{34}^2 &\sim (\Gamma_3 + \Gamma_4) c t^0; \\ r_{13}^2 &\sim -\Gamma_2 \Gamma_4 a b t^{2q}, & r_{24}^2 &\sim -\Gamma_1 \Gamma_3 a b t^{2q}; \\ r_{14}^2 &\sim \Gamma_2 \Gamma_3 a b t^{2q}, & r_{23}^2 &\sim \Gamma_1 \Gamma_4 a b t^{2q}; \\ (\Gamma_1 + \Gamma_2)(\Gamma_3 + \Gamma_4) &\neq 0, & c^2 &= -\frac{\Gamma_1 \Gamma_2}{\Gamma_3 \Gamma_4}. \end{aligned} \quad (4.20)$$

### 4.3.2 Diagram II

For Diagram II, it is obvious that  $z_{kl} \approx t^{\gamma-q}$ ,  $w_{kl} \approx t^{-\gamma-q}$  for any  $(k, l)$ ,  $1 \leq k < l \leq 4$ . Thus we can assume that

$$z_{kl} \sim a_{kl} t^{\gamma-q}, \quad w_{kl} \sim b_{kl} t^{-\gamma-q}.$$

By

$$z_n = \sum_{j \neq n} \Gamma_j Z_{jn}, \quad w_n = \sum_{j \neq n} \Gamma_j W_{jn}, \quad n = 1, 2, 3,$$

it follows that

$$\begin{aligned} \frac{\Gamma_2}{a_2 - a_1} + \frac{\Gamma_3}{a_3 - a_1} + \frac{\Gamma_4}{a_4 - a_1} &= 0, \\ \frac{\Gamma_1}{a_1 - a_2} + \frac{\Gamma_3}{a_3 - a_2} + \frac{\Gamma_4}{a_4 - a_2} &= 0, \\ \frac{\Gamma_1}{a_1 - a_3} + \frac{\Gamma_2}{a_2 - a_3} + \frac{\Gamma_4}{a_4 - a_3} &= 0; \\ \frac{\Gamma_2}{b_2 - b_1} + \frac{\Gamma_3}{b_3 - b_1} + \frac{\Gamma_4}{b_4 - b_1} &= 0, \\ \frac{\Gamma_1}{b_1 - b_2} + \frac{\Gamma_3}{b_3 - b_2} + \frac{\Gamma_4}{b_4 - b_2} &= 0, \\ \frac{\Gamma_1}{b_1 - b_3} + \frac{\Gamma_2}{b_2 - b_3} + \frac{\Gamma_4}{b_4 - b_3} &= 0. \end{aligned}$$

On the other hand, by  $S = 0$  it follows that

$$\sum_{1 \leq j < k \leq 4} \Gamma_j \Gamma_k a_{jk} b_{jk} = 0.$$

A straightforward computation shows that there is no solution for the above equations except the case that

$$\Gamma_i = \Gamma_j = \Gamma_k = -\Gamma_l,$$

where  $(ijkl)$  is a certain permutation of  $\{1, 2, 3, 4\}$ .

Therefore, Diagram II is impossible except perhaps for the case that three of vorticities are equal and the fourth vorticity is opposite of them.

Note that, when Diagram II is possible, we have

$$r_{kl} \approx t^{-q}, \quad 1 \leq k < l \leq 4, \quad (4.21)$$

in particular,

$$\frac{r_{ij}}{r_{kl}} \approx t^0, \quad (4.22)$$

where  $(ijkl)$  is any permutation of  $\{1, 2, 3, 4\}$ .

### 4.3.3 Diagram III

For Diagram III we can assume that

$$\begin{aligned} z_1 \sim z_4 \sim -\Gamma_2 at^q, & \quad z_2 \sim z_3 \sim \Gamma_1 at^q, \\ w_1 \sim w_2 \sim -\Gamma_4 bt^q, & \quad w_3 \sim w_4 \sim \Gamma_1 bt^q. \end{aligned}$$

It follows that

$$\Gamma_1 \Gamma_3 = \Gamma_2 \Gamma_4.$$

Moreover, similar to Subsection 5.3 in [16], it is easy to see that

$$(\Gamma_1 + \Gamma_2)(\Gamma_2 + \Gamma_3)(\Gamma_3 + \Gamma_4)(\Gamma_1 + \Gamma_4) \neq 0.$$

By  $L = 0$ , it follows that

$$\Gamma_1 \Gamma_3 = \Gamma_2 \Gamma_4 < 0.$$

Obviously,

$$z_{12} \sim (\Gamma_1 + \Gamma_2) at^q.$$

By  $z_2 \sim \Gamma_1 \frac{1}{\Lambda w_{12}}$ , it follows that

$$w_{12} \sim \frac{1}{ac} t^{-\gamma-q}.$$

Similarly,

$$\begin{aligned} z_{13} \sim (\Gamma_1 + \Gamma_2) at^q, & \quad w_{13} \sim (\Gamma_1 + \Gamma_4) bt^q, \\ z_{14} \sim \frac{c}{b} t^{\gamma-q}, & \quad w_{14} \sim (\Gamma_1 + \Gamma_4) bt^q, \\ z_{23} \sim \frac{a\Gamma_3}{b\Gamma_4} t^{\gamma-q}, & \quad w_{23} \sim (\Gamma_1 + \Gamma_4) bt^q, \\ z_{24} \sim -(\Gamma_1 + \Gamma_2) at^q, & \quad w_{24} \sim (\Gamma_1 + \Gamma_4) bt^q, \\ z_{34} \sim -(\Gamma_1 + \Gamma_2) at^q, & \quad w_{34} \sim -\frac{\Gamma_3}{ac\Gamma_2} t^{-\gamma-q}. \end{aligned}$$

Note that, when Diagram III is possible, we have

$$r_{12} \approx r_{34} \approx t^{-\frac{\gamma}{2}}, \quad r_{13} \approx r_{24} \approx t^q, \quad r_{23} \approx r_{14} \approx t^{\frac{\gamma}{2}}, \quad (4.23)$$

in particular,

$$\frac{r_{ij}}{r_{kl}} \approx t^0, \quad (4.24)$$

where  $(ijkl)$  is any permutation of  $\{1, 2, 3, 4\}$ .

## 5 Possible diagrams in the case $q = -|\gamma|/2$

In this section, we consider the case that  $q = -\frac{|\gamma|}{2}$ . Without loss of generality, we only consider the case that  $q = -\frac{\gamma}{2}$ .

If  $q = -\frac{\gamma}{2}$ , then for any  $(k, l)$ ,  $1 \leq k < l \leq 4$ , we have  $w_{kl} \approx t^{-\frac{\gamma}{2}}$ . Hence  $Z_{kl} \approx t^{-\frac{\gamma}{2}}$  also holds. Note that, for any  $(k, l)$ , vertices  $\mathbf{k}$  and  $\mathbf{l}$  form a  $z$ -stroke, but they are never  $w$ -close.

It is easy to see that

$$w_n \preceq t^{-\frac{\gamma}{2}} \text{ for } n = 1, 2, 3, 4.$$

### 5.1 The case that some $w_n \prec t^{-\frac{\gamma}{2}}$

If there is one  $w_n$ , say  $w_4$ , such that  $w_4 \prec t^{-\frac{\gamma}{2}}$ . Then, obviously,

$$w_1 \approx w_2 \approx w_3 \approx t^{-\frac{\gamma}{2}}.$$

Let us consider possible diagrams by Rules in Section 3.

#### 5.1.1 Possible diagrams

Obviously, all the possible diagrams contain three  $w$ -circles at vertices  $\mathbf{1}, \mathbf{2}, \mathbf{3}$  and six  $z$ -strokes.

**Case 1: When there is no any  $w$ -stroke connected vertex  $\mathbf{4}$ .**

Then it is easy to see that vertices  $\mathbf{1}, \mathbf{2}, \mathbf{3}$  formed a  $w$ -color triangle by Rule I and Rule VI. Next, we classify all possible diagrams as follows:

- there is no any  $z$ -circle;
- $z$ -circle exists but there is no  $z$ -circle at vertex  $\mathbf{4}$ , then there are three  $z$ -circles at vertices  $\mathbf{1}, \mathbf{2}, \mathbf{3}$  by Rule II and Estimate 2 in Proposition 3.1;
- there is a  $z$ -circle at vertex  $\mathbf{4}$ , then there are also three  $z$ -circles at vertices  $\mathbf{1}, \mathbf{2}, \mathbf{3}$  by Rule IV and Estimate 2 in Proposition 3.1.

Thus the only possible diagrams are those in the following Figure 12.

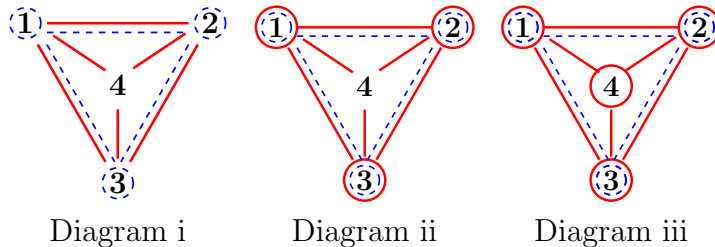


Figure 12

**Case 2: When there is some  $w$ -stroke connected vertex  $\mathbf{4}$ .**

Then it is easy to see that six  $w$ -strokes by Rule VI. Next, we classify all possible diagrams as follows:

- there is no any  $z$ -circle;
- $z$ -circle exists, then there are four  $z$ -circles at vertices **1,2,3,4** by Rule II and Estimate 2 in Proposition 3.1.

Thus the only possible diagrams are those in the following Figure 13.

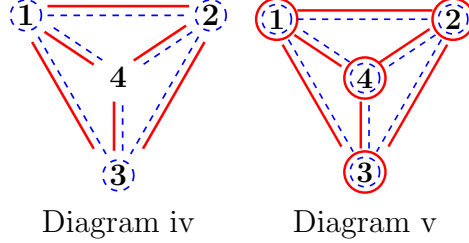


Figure 13

### 5.1.2 Exclusion of diagrams

**Case i:** For Diagram i we can assume that

$$w_4 \prec w_n \sim b_n t^{-\frac{\sigma}{2}}, \quad n = 1, 2, 3,$$

where  $b_n$  are three unequal nonzero numbers.

By

$$z_n = \sum_{j \neq n} \Gamma_j Z_{jn}, \quad n = 1, 2, 3,$$

it follows that

$$\begin{aligned} \frac{\Gamma_2}{b_2 - b_1} + \frac{\Gamma_3}{b_3 - b_1} + \frac{\Gamma_4}{-b_1} &= 0, \\ \frac{\Gamma_1}{b_1 - b_2} + \frac{\Gamma_3}{b_3 - b_2} + \frac{\Gamma_4}{-b_2} &= 0, \\ \frac{\Gamma_1}{b_1 - b_3} + \frac{\Gamma_2}{b_2 - b_3} + \frac{\Gamma_4}{-b_3} &= 0. \end{aligned}$$

A straightforward computation shows that there is no solution for the above equations except the case that  $\Gamma_1 = \Gamma_2 = \Gamma_3 = -\Gamma_4$ .

As a result, Diagram i is impossible except perhaps for the case that

$$\Gamma_1 = \Gamma_2 = \Gamma_3 = -\Gamma_4.$$

Note that, when Diagram i is possible, we have

$$\begin{aligned} r_{kl} &\approx t^{\frac{\sigma}{2}} = t^{-q}, & 1 \leq k < l \leq 3, \\ t^{-q} &\prec r_{j4} \prec t^q, & 1 \leq j \leq 3; \end{aligned} \quad (5.25)$$

in particular,

$$\frac{r_{kl}}{r_{j4}} \prec t^0 \prec \frac{r_{j4}}{r_{kl}}, \quad (5.26)$$

where  $(jkl)$  is any permutation of  $\{1, 2, 3\}$ .

**Case ii:** For Diagram ii it is easy to see that

$$z_4 \prec z_1 \sim z_2 \sim z_3.$$

By

$$\sum_{j=1}^4 \Gamma_j z_j = 0,$$

it follows that

$$\Gamma_1 + \Gamma_2 + \Gamma_3 = 0.$$

However, this relation is in conflict with  $L = 0$ .

As a result, Diagram ii is impossible.

**Case iii:** For Diagram iii, without loss of generality, , we can assume that

$$z_1 \sim z_2 \sim z_3 \sim -\Gamma_4 t^{-\frac{\gamma}{2}}, \quad z_4 \sim (\Gamma_1 + \Gamma_2 + \Gamma_3) t^{-\frac{\gamma}{2}}$$

By

$$w_4 = \sum_{k \neq 4} \Gamma_k Z_{k4},$$

it follows that

$$\frac{\Gamma_1}{\Gamma} + \frac{\Gamma_2}{\Gamma} + \frac{\Gamma_3}{\Gamma} = 0,$$

or

$$\Gamma_1 + \Gamma_2 + \Gamma_3 = 0.$$

However, this relation is in conflict with  $L = 0$ .

As a result, Diagram iii is impossible.

**Case iv:** For Diagram iv it is easy to see that the result is similar to Diagram i, i.e., Diagram iv is impossible except perhaps for the case that  $\Gamma_1 = \Gamma_2 = \Gamma_3 = -\Gamma_4$ .

Note that, when Diagram iv is possible, we have

$$r_{kl} \approx t^{\frac{\gamma}{2}} = t^{-q}, \quad 1 \leq k < l \leq 4; \quad (5.27)$$

in particular,

$$\frac{r_{ij}}{r_{kl}} \approx t^0, \quad (5.28)$$

where  $(ijkl)$  is any permutation of  $\{1, 2, 3, 4\}$ .

**Case v:** For Diagram v it is easy to see that

$$z_1 \sim z_2 \sim z_3 \sim z_4,$$

it follows that

$$\Gamma_1 + \Gamma_2 + \Gamma_3 + \Gamma_4 = 0.$$

However, this relation is in conflict with  $L = 0$ .

As a result, Diagram v is impossible.

## 5.2 The case that all $w_n \approx t^{-\frac{\gamma}{2}}$

If  $w_1 \approx w_2 \approx w_3 \approx w_4 \approx t^{-\frac{\gamma}{2}}$ .

Let us consider possible diagrams by Rules in Section 3.

### 5.2.1 Possible diagrams

Obviously, all the possible diagrams contain four  $w$ -circles and six  $z$ -strokes. Then, similar to the above subsection, it is easy to show that the following five diagrams in Figure 14 exhaust all the possible diagrams:

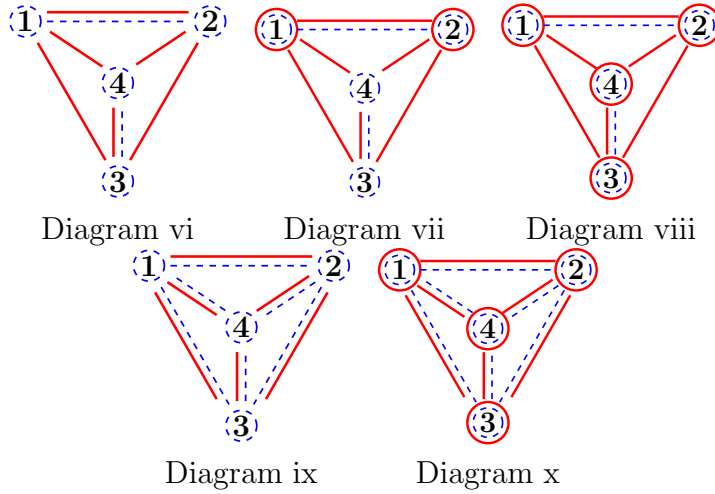


Figure 14: Possible diagrams for  $q = -\frac{\gamma}{2}$  and all  $w_n \approx t^{-\frac{\gamma}{2}}$

### 5.2.2 Exclusion of diagrams

**Case vi:** For Diagram vi we can assume that

$$\begin{aligned} w_1 &\sim -\Gamma_2 a t^{-\frac{\gamma}{2}}, & w_2 &\sim \Gamma_1 a t^{-\frac{\gamma}{2}}, \\ w_3 &\sim -\Gamma_4 b t^{-\frac{\gamma}{2}}, & w_4 &\sim \Gamma_3 b t^{-\frac{\gamma}{2}}. \end{aligned}$$

By

$$z_n = \sum_{j \neq n} \Gamma_j Z_{jn}, \quad n = 1, 2, 3,$$

it follows that

$$\begin{aligned} \frac{\Gamma_2}{-\Gamma_2 a - \Gamma_1 a} + \frac{\Gamma_3}{-\Gamma_2 a + \Gamma_4 b} + \frac{\Gamma_4}{-\Gamma_2 a - \Gamma_3 b} &= 0, \\ \frac{\Gamma_1}{\Gamma_1 a + \Gamma_2 a} + \frac{\Gamma_3}{\Gamma_1 a + \Gamma_4 b} + \frac{\Gamma_4}{\Gamma_1 a - \Gamma_3 b} &= 0, \\ \frac{\Gamma_1}{-\Gamma_4 b - \Gamma_1 a} + \frac{\Gamma_2}{-\Gamma_4 b - \Gamma_1 a} + \frac{\Gamma_4}{-\Gamma_4 b - \Gamma_3 b} &= 0. \end{aligned}$$

A straightforward computation shows that there is no solution for the above equations except the case  $\Gamma_3 = \Gamma_4 = (\sqrt{3} - 2)^{\pm 1} \Gamma_1 = (\sqrt{3} - 2)^{\pm 1} \Gamma_2$ .

Thus Diagram vi is impossible except perhaps for the case

$$\Gamma_3 = \Gamma_4 = (\sqrt{3} - 2)^{\pm 1} \Gamma_1 = (\sqrt{3} - 2)^{\pm 1} \Gamma_2.$$

Note that, when Diagram vi is possible, we have

$$\begin{aligned} r_{12} &\approx r_{34} \approx t^{\frac{\gamma}{2}} = t^{-q}, \\ t^{-q} &\prec r_{13}, r_{24}, r_{14}, r_{23} \prec t^q. \end{aligned} \tag{5.29}$$

**Case vii:** For Diagram vii we can assume that

$$w_1 \sim -\Gamma_2 a t^{-\frac{\gamma}{2}}, w_2 \sim \Gamma_1 a t^{-\frac{\gamma}{2}}.$$

However, it is easy to see that

$$z_1 \sim z_2 \approx t^{-\frac{\gamma}{2}},$$

thus we have  $\Gamma_1 + \Gamma_2 = 0$ . Then it is obvious that  $w_{12} \prec t^{-\frac{\gamma}{2}}$ , this is in conflict with  $w_{12} \approx t^{-\frac{\gamma}{2}}$ . As a result, Diagram vii is impossible.

**Case viii:** For Diagram viii we can assume that

$$\begin{aligned} w_1 &\sim -\Gamma_2 a t^{-\frac{\gamma}{2}}, & w_2 &\sim \Gamma_1 a t^{-\frac{\gamma}{2}}, \\ w_3 &\sim -\Gamma_4 b t^{-\frac{\gamma}{2}}, & w_4 &\sim \Gamma_3 b t^{-\frac{\gamma}{2}}, \\ z_1 &\sim z_2 \sim a' t^{-\frac{\gamma}{2}}, & z_3 &\sim z_4 \sim b' t^{-\frac{\gamma}{2}}. \end{aligned}$$

Note that

$$(\Gamma_1 + \Gamma_2)(\Gamma_3 + \Gamma_4) \neq 0,$$

and

$$b' = -(\Gamma_1 + \Gamma_2)a' / (\Gamma_3 + \Gamma_4).$$

By

$$w_{12} = (\Gamma_1 + \Gamma_2)W_{12} + \Gamma_3(W_{32} - W_{31}) + \Gamma_4(W_{42} - W_{41}),$$

it follows that

$$w_{12} = (\Gamma_1 + \Gamma_2) \frac{\Lambda}{z_{12}} + O(t^{\frac{7}{2}\gamma}),$$

or

$$z_{12} = \frac{(\Gamma_1 + \Gamma_2)\Lambda}{w_{12}} + O(t^{\frac{11}{2}\gamma}) \approx t^{\frac{3}{2}\gamma},$$

By

$$z_{12} = (\Gamma_1 + \Gamma_2)Z_{12} + \Gamma_3(Z_{32} - Z_{31}) + \Gamma_4(Z_{42} - Z_{41}),$$

it follows that

$$z_{12} = \frac{\Gamma_1 + \Gamma_2}{\Lambda w_{12}} - \Gamma_3 \frac{w_{12}}{\Lambda w_{13} w_{23}} - \Gamma_4 \frac{w_{12}}{\Lambda w_{41} w_{42}}.$$

Therefore,

$$\frac{\Gamma_1 + \Gamma_2}{w_{12}^2} \sim \frac{1}{w_{31} w_{32}} + \frac{1}{w_{14} w_{24}}.$$

Similarly, we also have

$$\frac{\Gamma_3 + \Gamma_4}{w_{34}^2} \sim \frac{1}{w_{13}w_{14}} + \frac{1}{w_{23}w_{24}}.$$

As a result, nonzero numbers  $a, b$  satisfy

$$\begin{aligned} \frac{\Gamma_1 + \Gamma_2}{a^2(\Gamma_1 + \Gamma_2)^2} &= \frac{1}{(-\Gamma_4 b + \Gamma_2 a)(-\Gamma_4 b - \Gamma_1 a)} + \frac{1}{(\Gamma_3 b + \Gamma_2 a)(\Gamma_3 b - \Gamma_1 a)}, \\ \frac{\Gamma_3 + \Gamma_4}{b^2(\Gamma_3 + \Gamma_4)^2} &= \frac{1}{(-\Gamma_4 b + \Gamma_2 a)(\Gamma_3 b + \Gamma_2 a)} + \frac{1}{(-\Gamma_4 b - \Gamma_1 a)(\Gamma_3 b - \Gamma_1 a)}. \end{aligned} \quad (5.30)$$

On the other hand, by

$$z_n = \sum_{j \neq n} \Gamma_j Z_{jn}, \quad n = 1, 2, 3, 4,$$

it follows that

$$\begin{aligned} ca' &= -\frac{\Gamma_2}{(\Gamma_1 + \Gamma_2)a} + \frac{\Gamma_3}{\Gamma_4 b - \Gamma_2 a} - \frac{\Gamma_4}{\Gamma_3 b + \Gamma_2 a}, \\ ca' &= \frac{\Gamma_1}{(\Gamma_1 + \Gamma_2)a} + \frac{\Gamma_3}{\Gamma_4 b + \Gamma_1 a} + \frac{\Gamma_4}{\Gamma_1 a - \Gamma_3 b}, \\ cb' &= \frac{\Gamma_1}{\Gamma_2 a - \Gamma_4 b} - \frac{\Gamma_2}{\Gamma_1 a + \Gamma_4 b} - \frac{\Gamma_4}{\Gamma_3 b + \Gamma_4 b}, \\ cb' &= \frac{\Gamma_1}{\Gamma_2 a + \Gamma_3 b} + \frac{\Gamma_2}{-\Gamma_1 a + \Gamma_3 b} + \frac{\Gamma_3}{\Gamma_3 b + \Gamma_4 b}. \end{aligned} \quad (5.31)$$

A straightforward computation shows that, if there is a solution for the equations (5.30) and (5.31), we have

$$(\Gamma_1 \Gamma_4 - \Gamma_2 \Gamma_3)(\Gamma_1 \Gamma_3 - \Gamma_2 \Gamma_4) = 0.$$

As a matter of fact, if we use an equivalent form of the system (2.10) (see [16] and (7.51) below), then it is easy to see that, by

$$F_z - \Lambda f_z = 0 \quad \text{and} \quad G_z + \Lambda g_z = 0,$$

it follows that

$$\begin{aligned} (\Gamma_1 + \Gamma_2) (\Gamma_3^2 + \Gamma_4^2) - (\Gamma_1^2 + \Gamma_2^2) (\Gamma_3 + \Gamma_4) &= 0, \\ \Gamma_1 \Gamma_2 (\Gamma_1 + \Gamma_2)^2 + \Gamma_3 \Gamma_4 (\Gamma_3 + \Gamma_4)^2 - (\Gamma_1 + \Gamma_2)^2 (\Gamma_3 + \Gamma_4)^2 &= 0. \end{aligned} \quad (5.32)$$

However, a straightforward computation shows that there is no solution for the equations (5.32) and  $L = 0$ .

As a result, Diagram viii is impossible.

**Case ix:** For Diagram ix it is easy to see that, for any  $(k, l)$ ,  $1 \leq k < l \leq 4$ , we have

$$z_{kl} \approx t^{\frac{3}{2}\gamma}, \quad w_{kl} \approx t^{-\frac{1}{2}\gamma}.$$

Therefore,

$$r_{kl} \approx t^{\frac{\gamma}{2}} = t^{-q}, \quad 1 \leq k < l \leq 4; \quad (5.33)$$

in particular,

$$\frac{r_{ij}}{r_{kl}} \approx t^0, \quad (5.34)$$

where  $(ijkl)$  is any permutation of  $\{1, 2, 3, 4\}$ .

**Case x:** For Diagram x, it is easy to see that

$$z_1 \sim z_2 \sim z_3 \sim z_4 \approx t^{-\frac{\gamma}{2}}.$$

Then we have

$$\Gamma_1 + \Gamma_2 + \Gamma_3 + \Gamma_4 = 0.$$

However, this relation is in conflict with  $L = 0$ . Thus Diagram x is impossible.

### 5.3 Problematic diagrams

In conclusion, we have derived a list of problematic diagrams consisting of Diagram i, Diagram iv, Diagram vi and Diagram ix in Figure 15.

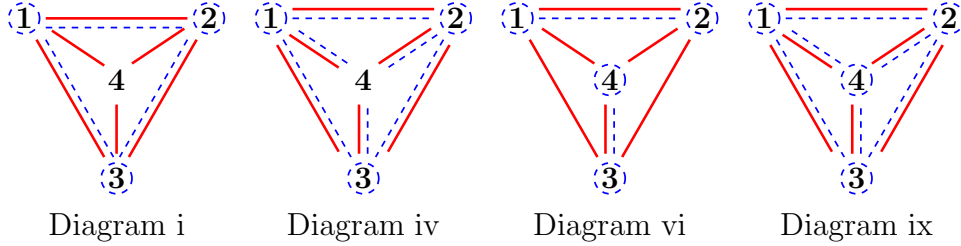


Figure 15: Problematic diagrams for  $q = -|\gamma|/2$

## 6 Finiteness results of collapse configurations

In this section we mainly prove the following result.

**Theorem 6.1** *If the vorticities  $\Gamma_n$  ( $n \in \{1, 2, 3, 4\}$ ) are nonzero, then the associated four-vortex problem has finitely many collapse configurations.*

Theorem 6.1 is an obvious inference of the following Theorems 6.4, 6.5 and 6.6. And we remark that the following results of finiteness are all on normalized collapse configurations in the complex domain, rather than real configurations.

First, we establish the following results.

**Lemma 6.2** *Any ratio  $r_{jk}^2/r_{lm}^2$  of two nonadjacent distances' squares is not dominating on the closed algebraic subset  $\mathcal{X}$  defined by the system (3.15).*

**Lemma 6.3** *Suppose the closed algebraic subset  $\mathcal{X}$  defined by the system (3.15) consists of infinitely many points. If all ratios  $r_{jk}^2/r_{lm}^2$  of two nonadjacent distances' squares are not dominating on the closed algebraic subset  $\mathcal{X}$ , Diagram I is impossible.*

*Proof of Lemma 6.2:*

If system (3.15) possesses infinitely many solutions, without lose of generality, assume that  $r_{12}^2/r_{34}^2$  is not dominating on the closed algebraic subset  $\mathcal{X}$ . Then some level set  $r_{12}^2/r_{34}^2 \equiv \text{const} \neq 0$ , denoted by  $\mathcal{X}_{lev}$ , also contains infinitely many points of  $\mathcal{X}$ .

On  $\mathcal{X}_{lev}$ , there is a Puiseux series as (3.16) with  $r_{12}^2(t)/r_{34}^2(t) = t$ . By considering the Puiseux series, it is obvious to see that only Diagram i and Diagram vi are possible.

**Case 1: If Diagram i occurs.**

Then, it is easy to show that, Diagram vi is impossible, and we have

$$\Gamma_1 = \Gamma_2 = \Gamma_3 = -\Gamma_4 \quad \text{or} \quad \Gamma_1 = \Gamma_2 = \Gamma_4 = -\Gamma_3.$$

By considering a Puiseux series as (3.16) with  $r_{12}^2(t)/r_{34}^2(t) = t^{-1}$ , it is easy to show that we have

$$\Gamma_3 = \Gamma_4 = \Gamma_1 = -\Gamma_2 \quad \text{or} \quad \Gamma_3 = \Gamma_4 = \Gamma_2 = -\Gamma_1.$$

However, the two requirements on vorticities above are not compatible with each other. This leads to a contradiction.

**Case 2: If Diagram vi occurs.**

Then, it is easy to show that, Diagram i is impossible, and we have

$$\Gamma_2 = \Gamma_4 = (\sqrt{3} - 2)^{\pm 1} \Gamma_1 = (\sqrt{3} - 2)^{\pm 1} \Gamma_3$$

or

$$\Gamma_2 = \Gamma_3 = (\sqrt{3} - 2)^{\pm 1} \Gamma_1 = (\sqrt{3} - 2)^{\pm 1} \Gamma_4.$$

Without loss of generality, assume vorticities satisfy

$$\Gamma_2 = \Gamma_4 = (\sqrt{3} - 2)^{\pm 1} \Gamma_1 = (\sqrt{3} - 2)^{\pm 1} \Gamma_3.$$

Then we are in one of diagrams in the following Figure 16.

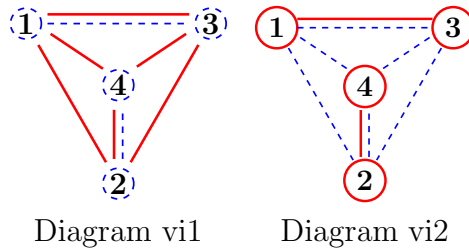


Figure 16: Complete problematic diagrams for  $\Gamma_2 = \Gamma_4 = (\sqrt{3} - 2)^{\pm 1} \Gamma_1 = (\sqrt{3} - 2)^{\pm 1} \Gamma_3$

For Diagram vi1 or Diagram vi2, we have

$$\frac{r_{13}^2}{r_{12}^2} \prec t^0,$$

thus  $\frac{r_{13}^2}{r_{12}^2}$  is dominating and there is a Puiseux series as (3.16) with  $\frac{r_{13}^2(t)}{r_{12}^2(t)} = t^{-1}$ . By considering the Puiseux series, it is obvious to see that Diagram vi1 and Diagram vi2 are impossible. This leads to a contradiction.

This completes the proof of Lemma 6.2. □

*Proof of Lemma 6.3:*

First, by the condition that all ratios  $r_{jk}^2/r_{lm}^2$  of two nonadjacent distances' squares are not dominating, it is easy to see that Diagram i is impossible.

Next, if Diagram I is possible, without loss of generality, assume that we are in the diagram in Figure 17. Then, by the condition that all ratios  $r_{jk}^2/r_{lm}^2$  of two nonadjacent

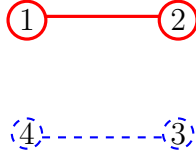


Figure 17: Diagram I

distances' squares are not dominating and by (4.20), it follows that

$$\begin{aligned} r_{34}^2 &= -\frac{\Gamma_1\Gamma_2(\Gamma_3+\Gamma_4)}{\Gamma_3\Gamma_4(\Gamma_1+\Gamma_2)}r_{12}^2, \\ r_{24}^2 &= \frac{\Gamma_1\Gamma_3}{\Gamma_2\Gamma_4}r_{13}^2, \\ r_{23}^2 &= \frac{\Gamma_1\Gamma_4}{\Gamma_2\Gamma_3}r_{14}^2. \end{aligned} \tag{6.35}$$

We claim that all ratios  $r_{jk}^2/r_{jl}^2$  of two adjacent distances' squares are dominating. Here we only prove that  $r_{13}^2/r_{14}^2$  is dominating. Otherwise,  $r_{13}^2/r_{14}^2 \equiv \text{const}$ , by (4.20), it is simple to see that

$$r_{13}^2/r_{14}^2 \equiv -\frac{\Gamma_1\Gamma_4}{\Gamma_1\Gamma_3}, \quad \text{or} \quad \Gamma_1\Gamma_3r_{13}^2 + \Gamma_1\Gamma_4r_{14}^2 = 0.$$

Therefore, by (6.35) and  $S = 0$ , it follows that

$$\Gamma_1\Gamma_2r_{12}^2 + \Gamma_3\Gamma_4r_{34}^2 = 0,$$

thus  $\Gamma_1 + \Gamma_2 + \Gamma_3 + \Gamma_4 = 0$ , but this is in conflict with  $L = 0$ . As a result,  $r_{13}^2/r_{14}^2$  is dominating. Similarly, it is easy to show that all ratios  $r_{jk}^2/r_{jl}^2$  of two adjacent distances' squares are dominating.

To prove that Diagram I is impossible, let us further consider a Puiseux series as (3.16) with  $\frac{r_{jk}^2(t)}{r_{jl}^2(t)} = t$  or with  $\frac{r_{jk}^2(t)}{r_{jl}^2(t)} = t^{-1}$ , it is easy to see that only Diagram I, Diagram III and Diagram vi are possible. Below by showing that these diagrams are impossible, we infer that Diagram I is impossible.

By considering  $\frac{r_{12}^2(t)}{r_{13}^2(t)} = t^{-1}$ , we are faced the following cases:

**Case 1: If Diagram I occurs.**

Then, it is easy to show that, we are in the diagram in Figure 18.

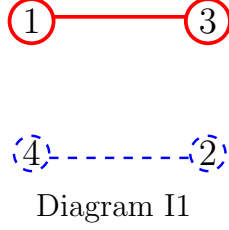


Figure 18: Problematic diagrams for Diagram I with  $r_{12}^2(t)/r_{13}^2(t) = t^{-1}$

For Diagram I1, it is easy to see that, vorticities satisfy

$$\begin{aligned} r_{24}^2 &= -\frac{\Gamma_1\Gamma_3(\Gamma_2+\Gamma_4)}{\Gamma_2\Gamma_4(\Gamma_1+\Gamma_3)}r_{13}^2, \\ r_{34}^2 &= \frac{\Gamma_1\Gamma_2}{\Gamma_3\Gamma_4}r_{12}^2, \\ r_{23}^2 &= \frac{\Gamma_1\Gamma_4}{\Gamma_2\Gamma_3}r_{14}^2. \end{aligned} \tag{6.36}$$

Then, by (6.35) and (6.36), it follows that

$$\Gamma_1 + \Gamma_2 + \Gamma_3 + \Gamma_4 = 0,$$

but this is in conflict with  $L = 0$ .

As a result, Diagram I does not occur.

**Case 2: If Diagram III occurs.**

Then, it is easy to show that, we are in one of diagrams in Figure 19.

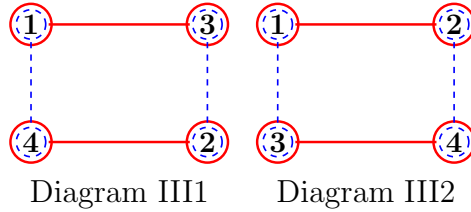


Figure 19: Problematic diagrams for Diagram III with  $r_{12}^2(t)/r_{13}^2(t) = t^{-1}$

For Diagram III1, it is easy to see that, vorticities satisfy

$$\begin{aligned} \Gamma_1\Gamma_2 &= \Gamma_3\Gamma_4, \\ r_{24}^2 &= \frac{\Gamma_2}{\Gamma_3}r_{13}^2, \\ r_{34}^2 &= -r_{12}^2, \\ r_{23}^2 &= \frac{\Gamma_2}{\Gamma_4}r_{14}^2. \end{aligned} \tag{6.37}$$

Then, by (6.35) and (6.37), it follows that

$$\Gamma_1 = \Gamma_2 = \Gamma_3 = \Gamma_4,$$

but this is in conflict with  $L = 0$ .

Similarly, for Diagram III2, we have

$$\begin{aligned}\Gamma_1\Gamma_4 &= \Gamma_2\Gamma_3, \\ r_{24}^2 &= \frac{\Gamma_4}{\Gamma_3}r_{13}^2, \\ r_{34}^2 &= \frac{\Gamma_4}{\Gamma_2}r_{12}^2, \\ r_{23}^2 &= -r_{14}^2.\end{aligned}\tag{6.38}$$

Then, by (6.35) and (6.37), it follows that

$$\Gamma_1\Gamma_4 = \Gamma_2\Gamma_3, \text{ and } \Gamma_1\Gamma_4 = -\Gamma_2\Gamma_3,$$

but this leads to a contradiction.

As a result, Diagram III does not occur.

**Case 3: If Diagram vi occurs.**

Then, it is easy to show that, we are in one of diagrams in Figure 20.

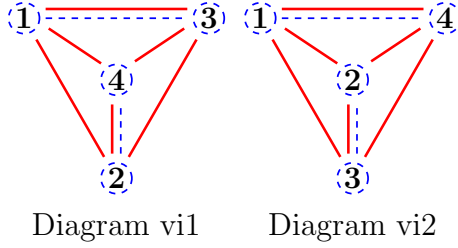


Figure 20: Problematic diagrams for Diagram vi with  $r_{12}^2(t)/r_{13}^2(t) = t^{-1}$

For these diagrams, we have

$$\Gamma_2 = \Gamma_4 = (\sqrt{3} - 2)^{\pm 1}\Gamma_1 = (\sqrt{3} - 2)^{\pm 1}\Gamma_3$$

or

$$\Gamma_2 = \Gamma_3 = (\sqrt{3} - 2)^{\pm 1}\Gamma_1 = (\sqrt{3} - 2)^{\pm 1}\Gamma_4.$$

Without loss of generality, assume vorticities satisfy

$$\Gamma_2 = \Gamma_4 = (\sqrt{3} - 2)^{\pm 1}\Gamma_1 = (\sqrt{3} - 2)^{\pm 1}\Gamma_3\tag{6.39}$$

Then we are in Diagram vi1.

By considering a Puiseux series as (3.16) with  $r_{13}^2(t)/r_{14}^2(t) = t^{-1}$ , once again, we are faced the following subcases:

**Subcase 1: If Diagram I occurs.**

Then, it is easy to show that, we are in the diagram in Figure 21.



Diagram I2

Figure 21: Problematic diagrams for Diagram I with  $r_{13}^2(t)/r_{14}^2(t) = t^{-1}$

For Diagram I2, it is easy to see that, vorticities satisfy

$$\begin{aligned} r_{23}^2 &= -\frac{\Gamma_1\Gamma_4(\Gamma_3+\Gamma_2)}{\Gamma_3\Gamma_2(\Gamma_1+\Gamma_4)}r_{14}^2, \\ r_{24}^2 &= \frac{\Gamma_1\Gamma_3}{\Gamma_2\Gamma_4}r_{13}^2, \\ r_{34}^2 &= \frac{\Gamma_1\Gamma_2}{\Gamma_4\Gamma_3}r_{12}^2. \end{aligned} \tag{6.40}$$

Then, by (6.35) and (6.40), it also follows that

$$\Gamma_1 + \Gamma_2 + \Gamma_3 + \Gamma_4 = 0,$$

but this is in conflict with  $L = 0$ .

As a result, Diagram I does not occur.

**Subcase 2: If Diagram III occurs.**

Then, it is easy to show that, we are in one of diagrams in Figure 22.

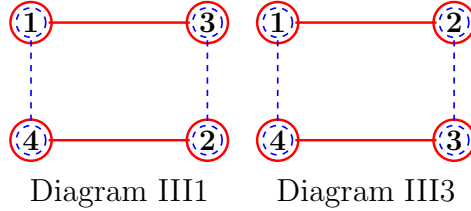


Figure 22: Problematic diagrams for Diagram III with  $r_{13}^2(t)/r_{14}^2(t) = t^{-1}$

For Diagram III1, we have shown that it is impossible.

For Diagram III3, we have

$$\begin{aligned} \Gamma_1\Gamma_3 &= \Gamma_2\Gamma_4, \\ r_{23}^2 &= \frac{\Gamma_3}{\Gamma_4}r_{14}^2, \\ r_{34}^2 &= \frac{\Gamma_3}{\Gamma_2}r_{12}^2, \\ r_{24}^2 &= -r_{13}^2. \end{aligned} \tag{6.41}$$

Then, by (6.35) and (6.41), it follows that

$$\Gamma_1\Gamma_3 = \Gamma_2\Gamma_4, \text{ and } \Gamma_1\Gamma_3 = -\Gamma_2\Gamma_4,$$

but this leads to a contradiction.

As a result, Diagram III does not occur.

**Subcase 3: If Diagram vi occurs.**

Then, it is easy to show that, we are in one of diagrams in Figure 23. For these

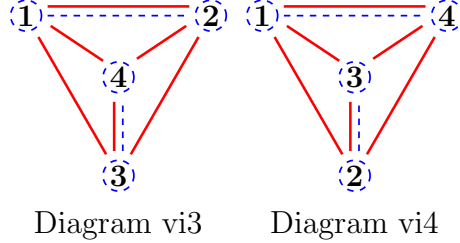


Figure 23: Problematic diagrams for Diagram vi with  $r_{13}^2(t)/r_{14}^2(t) = t^{-1}$

diagrams, we have

$$\Gamma_3 = \Gamma_4 = (\sqrt{3} - 2)^{\pm 1} \Gamma_1 = (\sqrt{3} - 2)^{\pm 1} \Gamma_2$$

or

$$\Gamma_2 = \Gamma_3 = (\sqrt{3} - 2)^{\pm 1} \Gamma_1 = (\sqrt{3} - 2)^{\pm 1} \Gamma_4.$$

However, the two requirements on vorticities above are both in conflict with (6.39). This leads to a contradiction.

As a result, Diagram vi does not occur in Case 3.

This completes the proof of Lemma 6.3. □

Therefore, we assume that all ratios of two nonadjacent distances' squares are constants, and Diagram I is impossible from now on. Note that Diagram i is also impossible by the condition that all ratios of two nonadjacent distances' squares are not dominating.

## 6.1 Finiteness of collapse configurations except two special cases

In this subsection we consider the finiteness problem of collapse configurations in the case that vorticities do not satisfy the following relations:

- $\Gamma_i = \Gamma_j = \Gamma_k = -\Gamma_l,$
- $\Gamma_i = \Gamma_j = (\sqrt{3} - 2)\Gamma_k = (\sqrt{3} - 2)\Gamma_l,$

where  $(ijkl)$  is a certain permutation of  $\{1, 2, 3, 4\}$ .

In this case only Diagram III and Diagram ix are possible.

**Theorem 6.4** *If the vorticities  $\Gamma_n$  ( $n \in \{1, 2, 3, 4\}$ ) are nonzero and do not satisfy any relation above, then the four-vortex problem has finitely many collapse configurations.*

**Proof.**

If there are infinitely many  $\Lambda \in \mathbb{S}$  such that equations (3.15) have a solution, then there is a Puiseux series as (3.16) with  $\Lambda(t) = t$ . By considering the Puiseux series, we are faced the following cases:

**Case 1: If we are in Diagram ix.**

Then, by (5.33), it follows that all products  $r_{jk}^2 r_{jl}^2$  of two adjacent distances' squares are dominating.

By considering a Puiseux series as (3.16) with  $r_{12}^2 r_{13}^2 = t^{-1}$ , we are in Diagram III, indeed, in one of diagrams in Figure 22.

Thus vorticities  $t$  satisfy the following relation.

$$(\Gamma_1 \Gamma_2 - \Gamma_3 \Gamma_4)(\Gamma_1 \Gamma_3 - \Gamma_2 \Gamma_4) = 0. \quad (6.42)$$

Similarly, by considering a Puiseux series as (3.16) with  $r_{12}^2 r_{14}^2 = t^{-1}$ , we have

$$(\Gamma_1 \Gamma_2 - \Gamma_3 \Gamma_4)(\Gamma_1 \Gamma_4 - \Gamma_2 \Gamma_3) = 0; \quad (6.43)$$

by considering a Puiseux series as (3.16) with  $r_{13}^2 r_{14}^2 = t^{-1}$ , we have

$$(\Gamma_1 \Gamma_3 - \Gamma_2 \Gamma_4)(\Gamma_1 \Gamma_4 - \Gamma_2 \Gamma_3) = 0. \quad (6.44)$$

Then, by (6.42), (6.43), (6.44) and  $L = 0$ , it follows that

$$\Gamma_i = \Gamma_j = (\sqrt{3} - 2)\Gamma_k = (\sqrt{3} - 2)\Gamma_l,$$

where  $(ijkl)$  is a certain permutation of  $\{1, 2, 3, 4\}$ . This leads to a contradiction.

As a result, Diagram ix is impossible.

**Case 2: We are in Diagram III.**

Without loss of generality, suppose we are in Diagram III1. Then, we have

$$\Gamma_1 \Gamma_2 - \Gamma_3 \Gamma_4 = 0, \quad (6.45)$$

and products  $r_{12}^2 r_{13}^2$  and  $r_{12}^2 r_{14}^2$  are dominating.

By considering a Puiseux series as (3.16) with  $r_{12}^2 r_{13}^2 = t$ , we are in the diagram in Figure 24. Therefore, we have

$$\Gamma_1 \Gamma_4 - \Gamma_2 \Gamma_3 = 0. \quad (6.46)$$

Similarly, by considering a Puiseux series as (3.16) with  $r_{12}^2 r_{14}^2 = t$ , we have

$$\Gamma_1 \Gamma_3 - \Gamma_2 \Gamma_4 = 0. \quad (6.47)$$

However, there is no solution for (6.45), (6.46), (6.47) and  $L = 0$ . This leads to a contradiction.

As a result, Diagram III is also impossible.

This completes the proof of Theorem 6.4. □

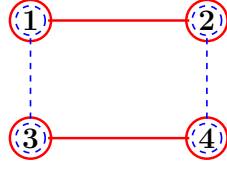


Figure 24: Problematic diagrams for Diagram III with  $r_{12}^2(t)r_{13}^2(t) = t$

## 6.2 Finiteness of collapse configurations in case $\Gamma_1 = \Gamma_2 = \Gamma_3 = -\Gamma_4$

In this subsection we consider the finiteness problem of collapse configurations in case that vorticities satisfy the following relation:

$$\Gamma_i = \Gamma_j = \Gamma_k = -\Gamma_l,$$

where  $(ijkl)$  is a certain permutation of  $\{1, 2, 3, 4\}$ . Without loss of generality, we only consider the case

$$\Gamma_1 = \Gamma_2 = \Gamma_3 = -\Gamma_4.$$

In this case only Diagram II, Diagram iv and Diagram ix are possible.

**Theorem 6.5** *If the vorticities  $\Gamma_n$  ( $n \in \{1, 2, 3, 4\}$ ) are nonzero and satisfy the relation  $\Gamma_1 = \Gamma_2 = \Gamma_3 = -\Gamma_4$ , then the four-vortex problem has finitely many collapse configurations.*

### Proof.

If there are infinitely many  $\Lambda \in \mathbb{S}$  such that equations (3.15) have a solution, then there is a Puiseux series as (3.16) with  $\Lambda(t) = t$ . By considering the Puiseux series, we are in Diagram II, Diagram iv or Diagram ix. However, all the three diagrams yield that

$$r_{kl} \approx t^{-q} \prec t^0, \quad 1 \leq k < l \leq 4.$$

It follows that  $r_{kl}^2$  are all dominating. Then, by considering a Puiseux series as (3.16) with  $r_{12}^2 = t^{-1}$ , it is easy to see that this contradicts the fact that  $r_{kl} \prec t^0$ . Consequently, we arrive at the conclusion that there are finitely many  $\Lambda \in \mathbb{S}$  such that equations (3.15) have a solution, the proof of Theorem 6.5 is now completed.  $\square$

## 6.3 Finiteness of collapse configurations in case $\Gamma_3 = \Gamma_4 = (\sqrt{3} - 2)\Gamma_1 = (\sqrt{3} - 2)\Gamma_2$

In this subsection we consider the finiteness problem of collapse configurations in case that vorticities satisfy the following relation:

$$\Gamma_i = \Gamma_j = (\sqrt{3} - 2)\Gamma_k = (\sqrt{3} - 2)\Gamma_l,$$

where  $(ijkl)$  is a certain permutation of  $\{1, 2, 3, 4\}$ . Without loss of generality, we only consider the case

$$\Gamma_3 = \Gamma_4 = (\sqrt{3} - 2)\Gamma_1 = (\sqrt{3} - 2)\Gamma_2. \quad (6.48)$$

In this case only Diagram III, Diagram vi and Diagram ix are possible.

**Theorem 6.6** *If the vorticities  $\Gamma_n$  ( $n \in \{1, 2, 3, 4\}$ ) are nonzero and satisfy the relation  $\Gamma_3 = \Gamma_4 = (\sqrt{3} - 2)\Gamma_1 = (\sqrt{3} - 2)\Gamma_2$ , then the four-vortex problem has finitely many collapse configurations.*

**Proof.**

If there are infinitely many  $\Lambda \in \mathbb{S}$  such that equations (3.15) have a solution, then there is a Puiseux series as (3.16) with  $\Lambda(t) = t$ . By considering the Puiseux series, we are in Diagram III, Diagram vi or Diagram ix.

We divide our proof in the following cases:

**Case 1: If we are in Diagram vi or Diagram ix.**

Then, by (5.29) and (5.33), it follows that all products of two adjacent distances' squares are dominating.

By considering a Puiseux series as (3.16) with  $r_{12}^2 r_{13}^2 = t^{-1}$ , we are in Diagram III, indeed, in one of diagrams in Figure 25.

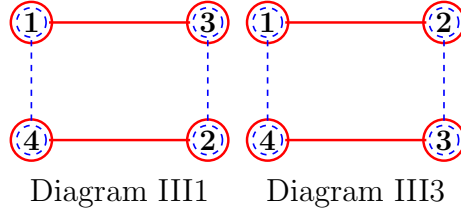


Figure 25: Problematic diagrams for Diagram III with  $r_{12}^2(t)r_{13}^2(t) = t^{-1}$

For Diagram III1, it follows that  $\Gamma_1\Gamma_2 = \Gamma_3\Gamma_4$ . This is in conflict with (6.48). Thus we are only in Diagram III3, it follows that

$$\begin{aligned} \Gamma_1\Gamma_3 &= \Gamma_2\Gamma_4, \\ r_{23}^2 &= \frac{\Gamma_3}{\Gamma_4}r_{14}^2, \\ r_{34}^2 &= \frac{\Gamma_3}{\Gamma_2}r_{12}^2, \\ r_{24}^2 &= -r_{13}^2. \end{aligned} \quad (6.49)$$

Similarly, by considering a Puiseux series as (3.16) with  $r_{12}^2 r_{14}^2 = t^{-1}$ , we are in Diagram III2 and it follows that

$$\begin{aligned} \Gamma_1\Gamma_4 &= \Gamma_2\Gamma_3, \\ r_{24}^2 &= \frac{\Gamma_4}{\Gamma_3}r_{13}^2, \\ r_{34}^2 &= \frac{\Gamma_4}{\Gamma_2}r_{12}^2, \\ r_{23}^2 &= -r_{14}^2. \end{aligned} \quad (6.50)$$

It is easy to see that (6.49) and (6.50) are in conflict with each other.

As a result, Diagram vi and Diagram ix are impossible. Therefore, by considering any Puiseux series as (3.16), we are only in Diagram III.

### Case 2: We are in Diagram III.

Without loss of generality, suppose we are in Diagram III3. Then, it follows that (6.49) holds, and products  $r_{12}^2 r_{13}^2$  and  $r_{13}^2 r_{14}^2$  are dominating.

By considering a Puiseux series as (3.16) with  $r_{12}^2 r_{13}^2 = t$ , we are in Diagram III2, and it follows that (6.50) holds. However, (6.49) and (6.50) are in conflict with each other.

As a result, Diagram III is also impossible.

Consequently, we arrive at the conclusion that there are finitely many  $\Lambda \in \mathbb{S}$  such that equations (3.15) have a solution, the proof of Theorem 6.6 is now completed.  $\square$

## 7 Upper bounds on the number of $\Lambda$ and on collapse configurations

In this section we provide upper bounds for the number of real normalized collapse configurations and for the number of the correlative  $\Lambda$ , mainly by making use of Bézout Theorem.

First, let us focus on the numbers of normalized collapse configurations and the correlative  $\Lambda$  in the complex domain. Recall that, normalized collapse configurations are characterized by nonzero solutions of the following equations such that  $\Lambda \in \mathbb{S} \setminus \{\pm 1\}$ .

$$\begin{cases} M_z = 0, & M_w = 0, \\ L = 0, & I = 0, & z_2 - z_1 = w_2 - w_1, \\ F_z - \Lambda f_z = 0, & \Lambda F_w - f_w = 0, \\ G_z + \Lambda g_z = 0, & \Lambda G_w + g_w = 0. \end{cases} \quad (7.51)$$

where

$$\begin{aligned} M_z &= \sum_{j=1}^4 \Gamma_j z_j, & M_w &= \sum_{j=1}^4 \Gamma_j w_j, \\ F_z &= \sum_{j=1}^4 \Gamma_j z_j^2 w_j, & f_z &= \sum_{1 \leq j < k \leq 4} \Gamma_j \Gamma_k (z_j + z_k), \\ F_w &= \sum_{j=1}^4 \Gamma_j z_j w_j^2, & f_w &= \sum_{1 \leq j < k \leq 4} \Gamma_j \Gamma_k (w_j + w_k), \\ G_z &= \Gamma_1 w_1 z_2 z_3 z_4 + \Gamma_2 w_2 z_1 z_3 z_4 + \Gamma_3 w_3 z_1 z_2 z_4 + \Gamma_4 w_4 z_1 z_2 z_3, \\ g_z &= \sum_{1 \leq j < k \leq 4, l < m, \{j,k,l,m\} = \{1,2,3,4\}} \Gamma_j \Gamma_k z_l z_m, \\ G_w &= \Gamma_1 z_1 w_2 w_3 w_4 + \Gamma_2 z_2 w_1 w_3 w_4 + \Gamma_3 z_3 w_1 w_2 w_4 + \Gamma_4 z_4 w_1 w_2 w_3, \\ g_w &= \sum_{1 \leq j < k \leq 4, l < m, \{j,k,l,m\} = \{1,2,3,4\}} \Gamma_j \Gamma_k w_l w_m. \end{aligned}$$

For more detail please refer to Subsection 7.2 in [16].

We now know that (7.51) has finitely many solutions in  $\Lambda, z, w$ . In the following, we focus on the solutions of (7.51) such that  $\Lambda \in \mathbb{S} \setminus \{\pm 1\}$  and  $(z, w) \neq (0, 0)$ .

For the system (7.51), by considering the map  $(z, w) \mapsto (\bar{z}, \bar{w})$ , one can prove that, the number of solutions associated with  $\Lambda$  is equal to the number of solutions associated with  $\bar{\Lambda}$  ( $= \Lambda^{-1}$ ). By considering the map  $(z, w) \mapsto (\mathbf{i}z, \mathbf{i}w)$ , one can prove that the number of solutions associated with  $\Lambda$  is equal to the number of solutions associated with  $-\Lambda$ .

Let  $\Lambda_j \in \mathbb{S}$  ( $j = 1, \dots, n_\Lambda$ ) be all points in the first quadrant associated with nonzero solutions of the system (7.51), and  $\mathcal{N}_{\Lambda_j}$  be the number of nonzero solutions (counting with the appropriate multiplicity) of the system (7.51) associated with  $\Lambda_j$ . Notations  $\mathcal{N}_{\bar{\Lambda}_j}$ ,  $\mathcal{N}_{-\Lambda_j}$ ,  $\mathcal{N}_{\mathbf{i}}$  and  $\mathcal{N}_{-\mathbf{i}}$  have similar meaning; but note that  $\mathcal{N}_{\mathbf{i}}$  and  $\mathcal{N}_{-\mathbf{i}}$  may be trivial, and yet

$$\mathcal{N}_{\Lambda_j} = \mathcal{N}_{\bar{\Lambda}_j} = \mathcal{N}_{-\Lambda_j} = \mathcal{N}_{-\bar{\Lambda}_j} \geq 2.$$

Indeed, by considering the map  $(z, w) \mapsto (-z, -w)$ , one can prove that every  $\mathcal{N}_{\Lambda_j}$  is an even number, so are  $\mathcal{N}_{\mathbf{i}}$  and  $\mathcal{N}_{-\mathbf{i}}$ . We also use notations  $\mathcal{N}_1$  and  $\mathcal{N}_{-1}$  to denote the number of nonzero solutions associated with  $\Lambda = 1$  and  $\Lambda = -1$ , respectively. We remark that  $\mathcal{N}_1$  and  $\mathcal{N}_{-1}$  are both even numbers, moreover,

$$\mathcal{N}_1 = \mathcal{N}_{-1} \geq 20,$$

since there are exactly 20 collinear nonzero solutions (counting with the appropriate multiplicity) when  $L = 0$ , please see Subsubsection 7.2.1 in [16] for more detail.

Let us embed the system (7.51) into a polynomial system in the projective space  $\mathbb{P}_{\mathbb{C}}^9$ :

$$\begin{cases} M_z = 0, & M_w = 0, \\ I = 0, & z_2 - z_1 = w_2 - w_1, \\ F_z - t\Lambda f_z = 0, & \Lambda F_w - t^3 f_w = 0, \\ G_z + t\Lambda g_z = 0, & \Lambda G_w + t^3 g_w = 0. \end{cases} \quad (7.52)$$

It is clear that the degree of the system (7.52) is no more than  $2 \times 3 \times 4 \times 4 \times 5 = 480$ .

To obtain an upper bound of the number of nonzero solutions for the system (7.51), let us estimate a lower bound of degree of the system (7.52) for three cases:

- $t = 0$  and  $\Lambda \neq 0$ ;
- $t \neq 0$  and  $\Lambda = 0$ ;
- $t = 0$  and  $\Lambda = 0$ .

**Case 1:  $t = 0$  and  $\Lambda \neq 0$ .**

Then the system (7.52) reduces to

$$\begin{cases} M_z = 0, & M_w = 0, \\ I = 0, & z_2 - z_1 = w_2 - w_1, \\ F_z = 0, & F_w = 0, \\ G_z = 0, & G_w = 0. \end{cases} \quad (7.53)$$

This system is an algebraic variety in  $\mathbb{P}_{\mathbb{C}}^7$  which is the same as the system (7.76) in [16] in form (note that  $L = 0$  here).

A straightforward computation similar to the one used for (7.76) in [16] shows that the degree of the system (7.53) is no less than  $6 \times 2 + 4 \times 2 = 20$ .

**Case 2:  $t \neq 0$  and  $\Lambda = 0$ .**

Then the system (7.52) reduces to

$$\begin{cases} M_z = 0, & M_w = 0, \\ I = 0, & z_2 - z_1 = w_2 - w_1, \\ F_z = 0, & f_w = 0, \\ G_z = 0, & g_w = 0. \end{cases} \quad (7.54)$$

This system is also an algebraic variety in  $\mathbb{P}_{\mathbb{C}}^7$ .

A straightforward computation shows that the variety (7.54) consists of a one-dimensional irreducible components (i.e., a one-dimensional lines):

$$w_1 = w_2 = w_3 = w_4 = 0, \quad M_z = 0, \quad z_2 - z_1 = 0.$$

Moreover, a straightforward computation shows that the multiplicity of this one-dimensional irreducible components is at least 2. It follows that the degree of the variety (7.54) is no less than 2.

**Case 3:  $t = 0$  and  $\Lambda = 0$ .**

Then the system (7.52) reduces to

$$\begin{cases} M_z = 0, & M_w = 0, \\ I = 0, & z_2 - z_1 = w_2 - w_1, \\ F_z = 0, & G_z = 0. \end{cases} \quad (7.55)$$

This system is also an algebraic variety in  $\mathbb{P}_{\mathbb{C}}^7$ .

A straightforward computation shows that the variety (7.55) consists of thirteen one-dimensional irreducible components (i.e., thirteen one-dimensional lines); moreover, a straightforward computation shows that the multiplicity of the irreducible component,

$$z_1 = z_2 = z_3 = z_4 = 0, \quad M_w = 0, \quad w_2 - w_1 = 0,$$

is at least 6.

Therefore, the degree of the variety (7.55) is no less than  $12 \times 1 + 1 \times 6 = 18$ .

Since the system (7.52) is a disjoint union of (7.51), (7.53), (7.54) and (7.55), it follows that the degree of the system (7.51) is no more than

$$480 - 20 - 2 - 18 = 440.$$

On the other hand, note that we have

**Proposition 7.1** *Assume  $L = 0$  and  $\Lambda \neq 0$ . If one solution of the system (7.51) satisfies  $z_j = z_k$  (or  $w_j = w_k$ ) for some  $j \neq k$ , then the solution is trivial.*

The Proposition is essentially Proposition 7.1 in [16], so the proof is omitted here. By Proposition 7.1, it follows that there is an isolated trivial solution of system (7.51) for any given  $\Lambda \neq 0$ . Moreover, it is easy to see that the multiplicity of this trivial solution is 8.

As a result, we have

$$4 \sum_{j=1}^{n_\Lambda} \mathcal{N}_{\Lambda_j} + \mathcal{N}_i + \mathcal{N}_{-i} + \mathcal{N}_1 + \mathcal{N}_{-1} \leq 440 - 8 = 432. \quad (7.56)$$

Based on this inequality, we have the following result.

**Corollary 7.1** *If the vorticities  $\Gamma_n$  ( $n \in \{1, 2, 3, 4\}$ ) are nonzero and satisfy  $L = 0$ , then the associated four-vortex problem has:*

- *at most 108 real central configurations*
- *at most 98 real collapse configurations*
- *at most 98  $\Lambda$  in  $\mathbb{S}$  associated with real collapse configurations*
- *at most 49 real collapse configurations for every  $\Lambda \in \mathbb{S} \setminus \{\pm 1, \pm i\}$ ; at most 98 real collapse configurations for every  $\Lambda \in \{\pm i\}$*
- *at most 216 central configurations in complex domain*
- *at most 196 collapse configurations in complex domain*
- *at most 196  $\Lambda$  in  $\mathbb{S}$  associated with collapse configurations in complex domain*
- *at most 49 collapse configurations in complex domain for every  $\Lambda \in \mathbb{S} \setminus \{\pm 1, \pm i\}$ ; at most 98 collapse configurations in complex domain for every  $\Lambda \in \{\pm i\}$ .*

**Proof.**

By (7.57), it follows that

$$4 \sum_{j=1}^{n_\Lambda} \mathcal{N}_{\Lambda_j} + \mathcal{N}_i + \mathcal{N}_{-i} \leq 392. \quad (7.57)$$

It is clear that

$$n_\Lambda \leq \begin{cases} \lfloor \frac{392}{8} \rfloor = 49, & \text{if } \mathcal{N}_i = 0; \\ \lfloor \frac{392-4}{8} \rfloor = 48. & \text{if } \mathcal{N}_i > 0. \end{cases}$$

Consequently, the number of  $\Lambda \in \mathbb{S} \setminus \{\pm 1\}$  such that the system (7.51) has nonzero solutions is no more than 196.

It is also clear that

$$\mathcal{N}_{\Lambda_j} \leq \lfloor \frac{392}{4} \rfloor = 98, \quad \mathcal{N}_i = \mathcal{N}_{-i} \leq \lfloor \frac{392}{2} \rfloor = 196. \quad (7.58)$$

Recall that, two solutions  $(\Lambda, z, w)$ ,  $(\Lambda, -z, -w)$  of the system (7.51) correspond to a same central configuration in complex domain. Therefore, in complex domain, by (7.56), there are at most 216 central configurations; by (7.57), there are at most 196 collapse configurations and at most 196  $\Lambda$  in  $\mathbb{S} \setminus \{\pm 1\}$  associated with collapse configurations; by (7.58), there are at most 49 collapse configurations for every  $\Lambda \in \mathbb{S} \setminus \{\pm 1, \pm \mathbf{i}\}$  and at most 98 collapse configurations for every  $\Lambda \in \{\pm \mathbf{i}\}$ .

Moreover, by considering the map  $(z, w) \mapsto (\mathbf{i}z, \mathbf{i}w)$ , it is easy to see that the total number of real collapse configurations for the system (7.51) corresponding to  $\Lambda_j$  and that associated with  $-\Lambda_j$  is no more than  $\lfloor \frac{N_{\Lambda_j}}{2} \rfloor$ ; the total number associated with  $\Lambda = \mathbf{i}$  or  $-\mathbf{i}$  is no more than  $\lfloor \frac{N_{\mathbf{i}}}{2} \rfloor$ ; the total number associated with  $\Lambda = 1$  or  $-1$  is no more than  $\lfloor \frac{N_1}{2} \rfloor$ .

As a result, by (7.56), there are at most 108 real central configurations; by (7.57), there are at most 98 real collapse configurations and at most 98  $\Lambda$  in  $\mathbb{S} \setminus \{\pm 1\}$  associated with real collapse configurations; by (7.58), there are at most 49 real collapse configurations for every  $\Lambda \in \mathbb{S} \setminus \{\pm 1, \pm \mathbf{i}\}$  and at most 98 real collapse configurations for every  $\Lambda \in \{\pm \mathbf{i}\}$ .

The proof is completed. □

## 8 Conclusion

To summarize, the main result Theorem 1.3 obviously follows from Theorem 1.1 and Theorem 6.1; and Corollary 1.4 follows from Corollary 1.2 and Corollary 7.1.

We conclude the paper by showing that the five-vortex problem has a continuum of collapse configurations. To this aim, let us consider one of four one-parameter families of real configurations such that

$$z_1 = -z_2 = a, \quad z_3 = -z_4 = b + \mathbf{i}c, \quad z_5 = 0;$$

where

$$b = \pm \sqrt{\frac{144a^6 - 121a^2}{64a^4 - 20}}, \quad c = \pm \sqrt{2a^2 - \frac{144a^6 - 121a^2}{64a^4 - 20}},$$

and

$$a \in \left(-\frac{3}{2}, -\frac{\sqrt{\frac{11}{3}}}{2}\right) \cup \left(\frac{\sqrt{\frac{11}{3}}}{2}, \frac{3}{2}\right).$$

Then the vortices **1, 2, 3, 4** form a parallelogram, and the vortex **5** is located at the central position (see Figure 26).

A straightforward computation shows that the family of configurations above satisfies (2.6) if

$$\Gamma_1 = \Gamma_2 = 1, \quad \Gamma_3 = \Gamma_4 = -\frac{1}{2}, \quad \Gamma_5 = \frac{3}{4},$$

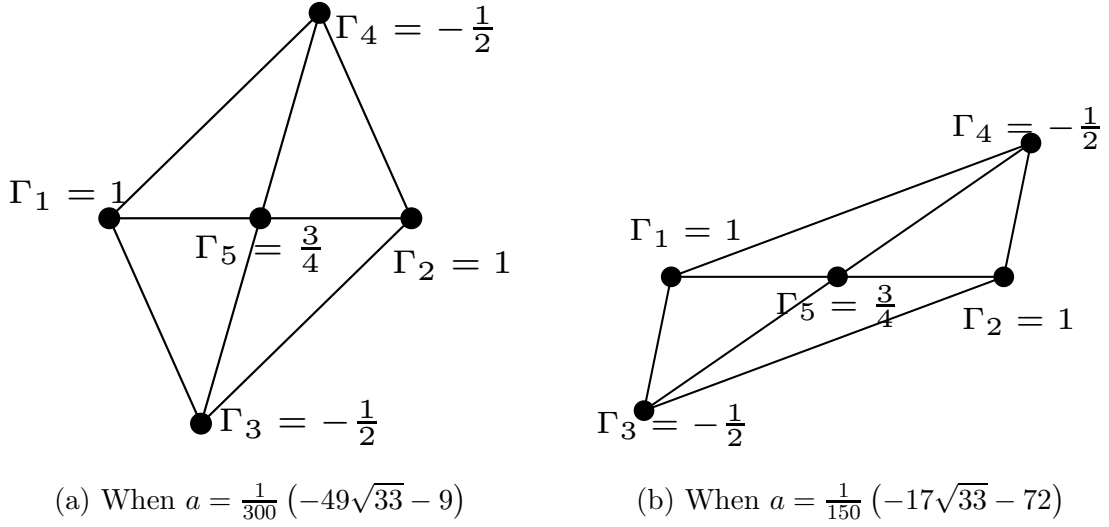


Figure 26: A one-parameter family of collapse configurations

and

$$\Lambda = \frac{-a^2 + 5b^2 - 10ibc - 5c^2}{2a^2(b^2 - 4ibc - 3c^2)}.$$

Note that

$$|\Lambda| = 1 \quad \text{and} \quad \Lambda \notin \mathbb{R},$$

thus the family of configurations above is a continuum of real normalized collapse configurations in the five-vortex problem.

## References

- [1] A. Albouy and V. Kaloshin. Finiteness of central configurations of five bodies in the plane. *Annals of Mathematics*, 176(1):535–588, 2012.
- [2] H. Aref. Motion of three vortices. *The Physics of Fluids*, 22(3):393–400, 1979.
- [3] H. Aref. Integrable, chaotic, and turbulent vortex motion in two-dimensional flows. *Annual Review of Fluid Mechanics*, 15:345–389, 1983.
- [4] H. Aref and M. van Buren. Vortex triple rings. *Physics of fluids*, 17(5):057104, 2005.
- [5] D. Eisenbud and J. Harris. *3264 and all that: A second course in algebraic geometry*. Cambridge University Press, 2016.
- [6] W. Fulton. *Intersection theory*, volume 2. Springer Science & Business Media, 2013.
- [7] W. Gröbli. *Spezielle Probleme über die Bewegung geradliniger paralleler Wirbelfäden*, volume 8. Druck von Zürcher und Furrer, 1877.

- [8] M. Hampton and R. Moeckel. Finiteness of stationary configurations of the four-vortex problem. *Transactions of the American Mathematical Society*, 361(3):1317–1332, 2009.
- [9] M. Hampton and R. Moeckel. Finiteness of relative equilibria of the four-body problem. *Inventiones mathematicae*, 163(2):289–312, 2006.
- [10] H. Helmholtz. Über integrale der hydrodynamischen gleichungen, welche den wirbelbewegungen entsprechen. *Journal für die reine und angewandte Mathematik*, 1858(55):25–55, 1858.
- [11] E. A. Novikov and Yu. B. Sedov. Vortex collapse. *Zhurnal Eksperimentalnoi i Teoreticheskoi Fiziki*, 77:588–597, 1979.
- [12] K. A. O’Neil. Stationary configurations of point vortices. *Transactions of the American Mathematical Society*, 302(2):383–425, 1987.
- [13] K. A. O’Neil. Relative equilibrium and collapse configurations of four point vortices. *Regular and Chaotic Dynamics*, 12(2):117–126, 2007.
- [14] D. P. Patil and W. Vogel. Remarks on the algebraic approach to intersection theory. *Monatshefte für Mathematik*, 96(3):233–250, 1983.
- [15] J. L. Synge. On the motion of three vortices. *Canadian Journal of Mathematics*, 1(3):257–270, 1949.
- [16] Xiang Yu. Finiteness of stationary configurations of the planar four-vortex problem. *arXiv preprint arXiv:2103.06037*, 2021.